Minimal geodesics along volume preserving maps, through semi-discrete optimal transport

Quentin Mérigot, Jean-Marie Mirebeau

Minimal geodesics along volume preserving maps, through semi-discrete optimal transport

Quentin Mérigot[*][†]   Jean-Marie Mirebeau[*][‡]

August 30, 2016

Abstract

We introduce a numerical method for extracting minimal geodesics along the group of volume preserving maps, equipped with the L^2 metric, which as observed by Arnold [Arn66] solve the Euler equations of inviscid incompressible fluids. The method relies on the generalized polar decomposition of Brenier [Bre91], numerically implemented through semi-discrete optimal transport. It is robust enough to extract non-classical, multi-valued solutions of Euler's equations, for which the flow dimension - defined as the quantization dimension of Brenier's generalized flow - is higher than the domain dimension, a striking and unavoidable consequence of this model [Shn94]. Our convergence results encompass this generalized model, and our numerical experiments illustrate it for the first time in two space dimensions.

1   Introduction

The motion of an inviscid incompressible fluid, moving in a compact domain $X \subseteq \mathbb{R}^d$, is described by the Euler equations [Eul65]

$$\partial_t v + (v \cdot \nabla)v = -\nabla p \qquad\qquad \operatorname{div} v = 0, \qquad (1)$$

coupled with the impervious boundary condition $v \cdot n = 0$ on $\partial\Omega$. Here v denotes the fluid velocity, and p the pressure acts as a Lagrange multiplier for the incompressibility constraint. As observed by Arnold [Arn66], Euler equations (1) yield in Lagrangian coordinates the geodesic equations along the group SDiff of diffeomorphisms of X with unit jacobian, equipped with the L^2 metric. Indeed, let $s : [0, 1] \to$ SDiff be a smooth time dependent family of diffeomorphisms of X, describing the evolution over time of the position of the fluid particles. The position of the particle emanating from x at time t will be denoted indifferently $s_t(x)$ or $s(t, x)$, while the diffeomorphism at time t is denoted $s(t)$ or s_t. The Eulerian velocity v and acceleration a of the fluid particles are given by $v(t, s(t, x)) = \partial_t s(t, x)$ and $a(t, s(t, x)) = \partial_{tt} s(t, x)$. The jacobian constraint $\det \nabla s = 1$ yields $\operatorname{div} v = 0$, whereas the equation of geodesics on SDiff merely states that acceleration is a gradient, $a(t, x) = -\nabla p(t, x)$, which is equivalent to (1, Left). This formalism leads to two natural problems for Euler equations:

- The Cauchy problem, forward in time: given the initial position and velocity of the fluid particles, find their subsequent positions at all positive times. This amounts to computing the exponential map on the lie group SDiff.

[*]CNRS, Université Paris-Dauphine, UMR 7534, CEREMADE, Paris, France.
[†]ANR grant TOMMI, ANR-11-BS01-014-01
[‡]ANR grant NS-LBR, ANR-13-JS01-0003-01

- The boundary value problem: given some observed initial and final positions of the fluid particles, find their intermediate states. This amounts to computing a minimizing geodesic on SDiff.

This manuscript is devoted to the boundary value problem only. More precisely, consider an inviscid incompressible fluid flowing during the time interval $[0, 1]$, and a map $s^* : X \to X$ giving the final position $s^*(x)$ of each fluid particle initially at position $x \in X$. In this paper, we introduce a new numerical scheme for finding a minimizing geodesic joining the initial configuration $s_* = \mathrm{Id}$ to the final one s^*

$$\text{minimize} \int_0^1 \|\dot{s}(t)\|^2 dt, \qquad \text{subject to} \quad \begin{cases} \forall t \in [0, 1], \ s(t) \in \mathbb{S}, \\ s(0) = s_*, \ s(1) = s^*. \end{cases} \tag{2}$$

We denoted by $\mathbb{S} \subseteq L^2(X, \mathbb{R}^d)$ the space of maps preserving the Lebesgue measure on X, which in dimension $d \geq 3$ is the closure of SDiff. More formally, we let Leb denote the Lebesgue measure on X, rescaled so as to be a probability measure, and we let $f \# \mu$ denote the push-forward of a measure μ by a measurable map f, defined by $f \# \mu(A) := \mu(f^{-1}(A))$. Then the space $\mathbb{S}$ is the collection of measurable maps $s : X \to X$ obeying $s \# \mathrm{Leb} = \mathrm{Leb}$.

The motivation for this first relaxation — replacing SDiff with the closed subset $\mathbb{S}$ of L^2 — is that the optimized functional in (2) does not penalize the spatial derivatives of s, which are involved in the unit jacobian constraint defining SDiff. Despite this relaxation, the optimization problem (2) needs not have a minimizer in $s \in H^1([0, 1], \mathbb{S})$ in dimension $d \geq 3$ [Shn94], and minimizing sequences $(s_n)_{n \in \mathbb{N}}$ may instead display oscillations reminiscent of an homogeneization phenomenon. A second relaxation is therefore necessary, see [FD12] for a review.

Generalized flows Brenier introduced in [Bre89] a second relaxation of the minimizing geodesic problem (2) based on generalized flows, which allow particles to split and their paths to cross. This surprising behavior is an unavoidable consequence of the lack of viscosity in Euler's equations, which amounts to an infinite Reynolds number. Generalized flows are also relevant in dimension $d \in \{1, 2\}$ if the underlying physical model actually involves a three dimensional domain $X \times [0, \varepsilon]^{3-d}$ in which one neglects the fluid acceleration in the extra dimensions [Bre08]. Consider the space of continuous paths (of fluid particles)

$$\Omega := C^0([0, 1], X).$$

A *generalized flow*, in Brenier's sense [Bre89], is a probability measure μ over the space Ω of paths. We denote by $\mathrm{e}_t(\omega) := \omega(t)$ the evaluation map at time $t \in [0, 1]$. Given a generalized flow $\mu \in \mathrm{Prob}(\Omega)$, the pushforward measure $\mathrm{e}_t \# \mu$ can be understood as the distribution of particles at time t under the flow. The generalized flow is *incompressible* if for every time $t \in [0, 1]$, $\mathrm{e}_t \# \mu$ coincides with the uniform probability measure on the domain X. Rescaling the domain if necessary we assume that X has unit area, so that the uniform probability measure Leb is simply the restriction of the Lebesgue measure to X.

The use of generalized flows turns the highly non-linear incompressibility constraint $s(t) \in \mathbb{S}$ into a linear constraint $\mathrm{e}_t \# \mu = \mathrm{Leb}$. Note the similarity with Kantorovich's linearization of the non-linear mass preservation constraint in Monge's optimal transport problem. This idea leads to a convex relaxation of the minimizing geodesic distance problem (2), linearizing both
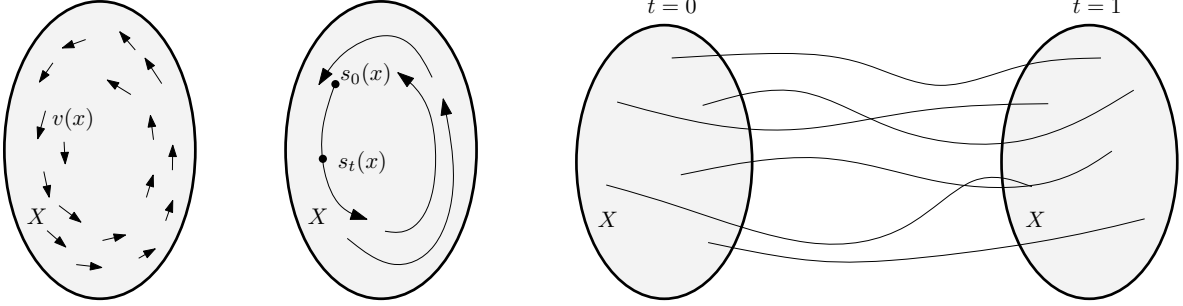
Figure 1: The motion of inviscid incompressible fluids admits three formulations, either (I) Eulerian based on the local speed $v : [0,1] \times X \to \mathbb{R}^d$, (II) Lagrangian based on diffeomorphisms $s(t, \cdot)$ which integrate the speed: $\partial_t s(t,x) = v(t, s(t,x))$, or (III) relaxed as a superposition of individual particles paths $\omega \in \Omega$, weighted by a measure μ.

the objective and the constraints, and for which the existence of a minimizer is guaranteed:

$$d^2(s_*, s^*) := \min_{\mu \in \text{Prob}(\Omega)} \int_\Omega \mathcal{A}(\omega) d\mu(\omega), \qquad \text{where } \mathcal{A}(\omega) = \int_0^1 |\dot{\omega}(t)|^2 dt$$

$$\text{and subject to } \begin{cases} \forall t \in [0,1], \ \text{e}_t \# \mu = \text{Leb}, \\ (\text{e}_0, \text{e}_1) \# \mu = (s_*, s^*) \# \text{Leb} . \end{cases} \tag{3}$$

As explained above, the first constraint in (3) expresses the incompressibility of the generalized flow. The second constraint $(\text{e}_0, \text{e}_1) \# \mu = (s_*, s^*) \# \text{Leb}$ rephrases the prescription of the end-points ($s(0) = s_*$ and $s(1) = s^*$) in the minimizing geodesic problem (2) by imposing a coupling between particle positions at initial and final times. This second constraint can equivalently be phrased in term of test functions: for every $f \in C^0(X \times X, \mathbb{R})$ one has

$$\int_\Omega f(\omega(0), \omega(1)) \, d\mu(\omega) = \int_X f(s_*(x), s^*(x)) \, dx.$$

In other words, $\omega(1) = s^*(s_*^{-1}(\omega(0)))$ for μ-almost any particle path $\omega \in \Omega$. Any classical flow $s \in H^1([0,1], \mathbb{S})$ can be represented by a generalized flow μ_s, supported on the paths $\omega_x : t \mapsto s(t,x)$, weighted by the Lebesgue measure on $x \in X$. In this case, if $F : \Omega \to \mathbb{R}$ is a bounded and continuous functional (or a lower-semi-continuous non-negative functional such as $\mathcal{A}$) one has

$$\int_\Omega F(\omega) \, d\mu_s(\omega) = \int_X F(\omega_x) \, dx. \tag{4}$$

$$\text{In particular,} \quad \int_\Omega \mathcal{A}(\omega) \, d\mu_s(\omega) = \int_X \int_0^1 |\dot{s}(t,x)|^2 \, dt \, dx = \int_0^1 \|\dot{s}(t)\|^2 dt. \tag{5}$$

In other words, the μ-average of the particles paths energy, is the time average of the fluid kinetic energy. Note that in this paper, $\|\cdot\|$ stands for the $L^2(X, \mathbb{R}^n)$ norm, and $|\cdot|$ for the Euclidean norm on $\mathbb{R}^d$. Our discretization truly solves Brenier's relaxation (3), rather than Arnold's formulation (2), and convergence is established in this relaxed setting.

Pressure. The incompressibility constraint in (3) gives rise to a Lagrange multiplier, called the pressure and which generalises the field p in (1). Pressure turns out to be the *unique* maximizer
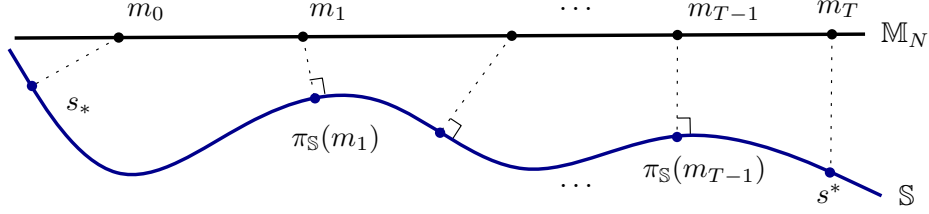
3

Figure 2: The geodesic distance $d^2(s_*, s^*)$ along the "manifold" $\mathbb{S}$ of volume preserving maps, represented as a blue curve, is estimated (9) as the length of a chain $(m_i)_{i=0}^T$ in the linear subspace $\mathbb{M}_N$, represented as a black line, plus penalizations for the boundary values and the distance from the chain elements to $\mathbb{S}$.

to a concave optimization problem dual to (3), see [Bre93]. Note that, in contrast, the primal problem (3) may have several minimizers — up to the notable exception [BFS09] of smooth flows in dimension $d = 1$. The pressure is a classical function $p \in L^2_{\text{loc}}(]0, 1[, \text{BV}(X))$, at least when the domain X is a d-dimensional torus [AF07]. This regularity is sufficient to show that any solution s to (2) (resp. μ-almost any path ω, for any solution μ to (3)) satisfies

$$\partial_{tt} s(t, x) = -\nabla p(t, s(t, x)), \qquad \text{resp.} \quad \ddot{\omega}(t) = -\nabla p(t, \omega(t)). \qquad (6)$$

This implies that the support of μ is contained in the space of solutions to a second-order Ordinary Differential Equation (ODE), a fact that we will use later in our convergence estimates. In other words, fluid particles move by inertia, only deflected by the force of pressure. Assume that the Hessian of the pressure is sufficiently small, namely that

$$\forall t \in [0, 1], \ \forall x \in X, \ \nabla^2 p(t, x) \prec \pi^2 \operatorname{Id} \qquad (7)$$

in the sense of symmetric matrices[1]. Then using the path dynamics equation (6) Brenier [Bre89] proved that the relaxed problem (3) admits a unique minimizer $\mu \in \text{Prob}(\Omega)$, which is *deterministic*. In other word, the generalized flow μ stems as in (4) from a possibly non-smooth but otherwise classical minimizer $s \in H^1([0, 1], \mathbb{S})$ of (2). Inequality (7) is sharp, and several families of examples are known for which uniqueness and/or determinism are lost precisely when the threshold (7) is passed. We present in §5 the first numerical illustration of this phenomenon.

1.1 Numerical scheme

We introduce a new discretization for the relaxation (3) of the shortest path formulation (2) of Euler equations (1). Our approach is numerically tractable in dimension 2, and is the first to illustrate the transition between classical and generalized solutions occurring at the threshold (7) on the pressure regularity.

For that purpose we need to introduce some notation. As before, we denote Leb the Lebesgue measure restricted to the domain X, which by assumption is a probability measure on X. Denote $\mathbb{M} := L^2(X, \mathbb{R}^d)$, and recall that $\mathbb{S} \subseteq \mathbb{M}$ is the collection of maps $s \in \mathbb{M}$ preserving the Lebesgue measure on the domain X, i.e. $s\#\text{Leb} = \text{Leb}$. For every $N \in \mathbb{N}$, we let $\mathcal{P}_N$ be a partition of X into N regions of equal area $1/N$, with respect to the Lebesgue measure, and with diameter $\leq C_\mathcal{P} N^{-\frac{1}{d}}$. Finally, we let $\mathbb{M}_N \subseteq \mathbb{M}$ be the N-dimensional subspace of functions which are piecewise constant over this partition. Given two measure-preserving maps $s_*, s^* \in \mathbb{S}$,

---

[1]We write $A \prec B$, where A and B are two symmetric matrices, if $B - A$ is positive definite.

discretization parameters $T, N \in \mathbb{N}$, and a penalization factor $\lambda \gg 1$, we introduce the functional which to $m \in \mathbb{M}_N^{T+1}$ associates

$$\mathcal{E}(T, N, \lambda; m) := T \sum_{0 \leq i < T} \|m_{i+1} - m_i\|^2 + \lambda \left(\|m_0 - s_*\|^2 + \|m_T - s^*\|^2 + \sum_{1 \leq i < T} d_\mathbb{S}^2(m_i) \right). \quad (8)$$

We denoted by $d_\mathbb{S}^2$ the squared-distance to the space $\mathbb{S}$ of measure-preserving maps, defined as usual by $d_\mathbb{S}^2(m) = \inf_{s \in \mathbb{S}} \|m - s\|^2$. Comparing this with (2), we recognize the standard discretization of the length of the discrete path $(m_0, \cdots, m_T)$, as well as an implementation by penalization of the boundary value constraints. The last term corresponds to a penalization of the incompressibility constraints, or more precisely a penalization of the squared distance between the maps m_i and the set $\mathbb{S}$ of measure preserving maps. The discrete optimization problem we consider is then

$$\mathcal{E}(T, N, \lambda) := \min_{m \in \mathbb{M}_N^{T+1}} \mathcal{E}(T, N, \lambda; m) \quad (9)$$

The problem (9), considered as a function of $m \in \mathbb{M}_N^{T+1}$, is an $N(T+1)d$-dimensional optimization problem. It makes sense to consider (8) and (9) whenever one attempts to approximate a shortest path joining two points s_*, s^* of a subset $\mathbb{S}$ of a Hilbert space $\mathbb{H}$, internally approximated by subspaces $(\mathbb{M}_N)_{N \geq 0}$. Our first result Proposition 1.1 uses no additional assumptions. In contrast, the numerical implementation strategy, and the other results §1.2, crucially rely on the specific properties of the set $\mathbb{S}$ of measure preserving maps.

The key properties of the functional (8) follow from those of the squared distance function $d_\mathbb{S}^2$, which are established in Proposition 5.1. It is continuously differentiable on an open dense set. However it is non-convex (in fact semi-concave) due to the non-convexity of the set $\mathbb{S}$, forbidding us to guarantee that the global minimum of (9) is found by our numerical solver. Nonetheless, our numerical experiments show that quasi-Newton methods give convincing results, see §5.

Distance to $\mathbb{S}$ and semi-discrete optimal transport. Before entering the analysis of (9), we want to emphasize that the inner-subproblems, namely the computation of the squared distances $d_\mathbb{S}^2(m_i)$, are numerically tractable thanks to two main ingredients: Brenier's polar factorization [Bre91], and semi-discrete optimal transport. Brenier's polar factorization theorem asserts that the distance between any $m \in \mathbb{M}$ and the set $\mathbb{S}$ of measure-preserving maps equals the cost of transporting the image measure $m\#\,\text{Leb}$ back to the Lebesgue measure, namely

$$d_\mathbb{S}^2(m) = \inf_{s \in \mathbb{S}} \|m - s\|^2 = W_2^2(m\#\,\text{Leb}, \text{Leb}), \quad (10)$$

where W_2 is the Wasserstein distance for the quadratic transport cost. Given any $m \in \mathbb{M}_N$, the pushforward measure $m\#\,\text{Leb}$ is the sum of N Dirac measures of mass $1/N$, located at the N values of the piecewise constant map m on the partition $\mathcal{P}_N$. Computing (10) therefore amounts to the computation of the Wasserstein distance between a finitely supported measure and the Lebesgue measure, a special instance of a problem called semi-discrete optimal transport. Efficient computational methods for this problem have been proposed [AHA98, Mer11, Lév14], relying on Kantorovich duality and on tools from computational geometry. Let η be the uniform probability measure over a finite set $Y \subseteq \mathbb{R}^d$ with cardinal N. Kantorovich duality asserts that

$$W_2^2(\eta, \text{Leb}) = \sup_{\substack{f:X \to \mathbb{R}, g:Y \to \mathbb{R} \\ f(x)+g(y) \leq \|x-y\|^2}} \int_X f(x) \, d\,\text{Leb}(x) + \int_X g(y) \, d\eta(y).$$

For any fixed $g : Y \to \mathbb{R}$ the largest $f : X \to \mathbb{R}$ obeying the constraint is given by

$$f(x) := \min_{y \in Y} \|x - y\|^2 - g(y).$$

This function is piecewise quadratic over a partition $(\mathrm{Lag}_y(g))_{y \in Y}$ of X into convex polyhedra

$$\mathrm{Lag}_y(g) := \left\{ x \in X \mid \forall z \in Y, \ \|x - y\|^2 - g(y) \leq \|x - z\|^2 - g(z) \right\}.$$

Eliminating the optimization variable f, Kantorovitch duality reads

$$W_2^2(\eta, \mathrm{Leb}) = \sup_{g : Y \to \mathbb{R}} \sum_{y \in Y} \int_{\mathrm{Lag}_y(g)} \left(\|x - y\|^2 - g(y) \right) dx + \frac{1}{N} \sum_{y \in Y} g(y). \tag{11}$$

This partition of X is called the Laguerre diagram of (Y, g) in computational geometry and can be computed in near-linear time in $\mathbb{R}^2$ using existing software[2] [cga]. Specifically, we use the 2D regular triangulations package in CGAL [Yvi13]. The maximization problem (11) is an unconstrained, concave and twice continuously differentiable maximization problem, which is efficiently solved via Newton or quasi-Newton methods. Semi-discrete optimal transport has become a reliable and efficient building block for PDE discretizations [BCMO14].

As discussed above, the chosen discretization of the Euler equations intrinsically leads to an optimal transport problem of semi-discrete type - from a finite collection of Diracs playing the role of fluid particles to the standard Lebesgue measure - hence our choice of discretization (11). A variety of alternative approaches have been developed for other instances of computational optimal transport, based for instance on a pressure-less fluid model [BBG02, PPO13], monotone discretizations of Monge-Ampere equation [BFO14, BCM14], regularization via entropy penalization [BCC+15, CPR15], or adaptive strategies for the linear programming discretization [OR15, Sch15].

1.2 Main results

Our results on the proposed discretization (8) are split into two parts. A convergence analysis first shows how to construct discrete generalized flows out of minimizers of $\mathcal{E}(T, N, \lambda)$, supported on finitely many piecewise linear paths and which converge to a solution $\mu \in \mathrm{Prob}(\Omega)$ of (3). This analysis requires upper bounds on the discrete energies $\mathcal{E}(T, N, \lambda)$, which are established in a second part and under adequate a-priori assumptions on the continuous solution. Importantly, two sets of assumptions are considered, encompassing the favorable case where a classical solution to Arnold's formulation (2) exists, and the general case where only Brenier's relaxation (3) is well posed.

Convergence analysis. We present two results establishing the convergence of the discretized problem (9) minimizers towards solutions of (3) as the number of timesteps T grows to infinity. The first proposition shows that one can build short chains of incompressible maps out of minimizers of (9). It involves the quantity

$$\mathcal{E}'(T, N, \lambda; m) := (1 + 4T/\lambda)\mathcal{E}(T, N, \lambda; m). \tag{12}$$

---

[2]In $\mathbb{R}^3$ the worst-case complexity of the Laguerre diagram is quadratic in the number of points, but this corresponds to degenerate cases, so that semi-discrete optimal can also be solved efficiently on $\mathbb{R}^3$ [Lév14].
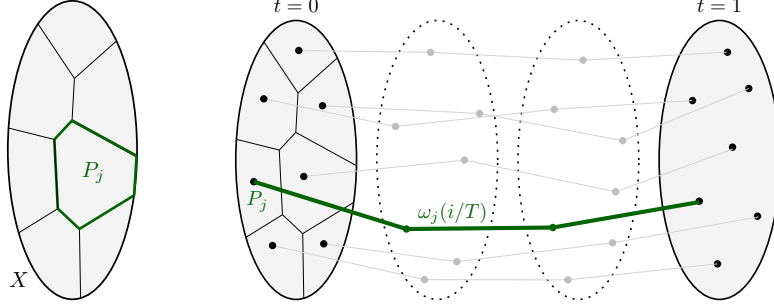
Figure 3: (Left) A partition $\mathcal{P}_N$ cuts the domain X into N region of equal area and roughly isotropic shape. (Right) To a sequence $(m_i)_{i=0}^T \in \mathbb{M}_N^{T+1}$ one can associate N piecewise linear paths $(\omega_j)_{j=1}^N$, by interpolating the map values at the times $\{0, 1/T, \cdots, T/T\}$ for each region of the partition $\mathcal{P}_N$.

Proposition 1.1. *Let* $m = (m_i)_{i=0}^T \in \mathbb{M}_N^{T+1}$ *and let* $(s_i)_{i=0}^T$ *be the chain of incompressible maps defined by:* $s_0 = s_*$, $s_T = s^*$, *and* s_i *is a projection of* m_i *onto* $\mathbb{S}$ *for all* $1 \leq i < T$. *Then*

$$T \sum_{0 \leq i < T} \|s_{i+1} - s_i\|^2 \leq \mathcal{E}'(T, N, \lambda; m).$$

Unfortunately, such discrete chains of incompressible maps need not converge as $T \to \infty$ to a continuous path $s : [0,1] \to \mathbb{S}$, due to the lack of compactness of $\mathbb{S}$. Note also that the interpolates $(1 - \delta)s_i + \delta s_{i+1}$, $0 \leq \delta \leq 1$, $0 \leq i \leq T$, need not belong to the non-convex set $\mathbb{S}$.

The next proposition establishes, under condition, convergence towards a solution of (3) in the sense of generalized flows, a framework which enjoys the desired convexity and compactness properties. In order to state this result, we associate to each $m = (m_i)_{i=0}^T$ in $\mathbb{M}_N^{T+1}$ a generalized flow $\mu_m \in \mathrm{Prob}(\Omega)$ uniformly supported on N paths. For every $j \in \{1, \ldots, N\}$, we denote m_i^j the (constant) value of m_i on the j-th region of the partition $\mathcal{P}_N$ of X and we define a path ω_j by interpolating linearly between these points, that is

$$\forall 0 \leq i \leq N, \ \omega_j(i/t) = m_i^j.$$

The construction of these paths is illustrated in Figure 3. Finally $\mu_m \in \mathrm{Prob}(\Omega)$ is the uniform probability measure over the finite set of paths $\{\omega_1, \ldots, \omega_N\} \subseteq \Omega$. We present in §2.2 a reformulation of the discrete energy (8) based on the generalized flow $\mu_m \in \mathrm{Prob}(\Omega)$, which mimics Brenier's linear relaxation (3) of Euler's equations.

Proposition 1.2. *Assume that* $\mathcal{E}'(T_k, N_k, \lambda_k; m_k) \to D_*$ *and* $T_k, N_k, \lambda_k \to +\infty$ *as* $k \to \infty$. *Then a subsequence of the generalized flows* μ_k *associated to* m_k *weak-* converges to a flow* $\mu \in \mathrm{Prob}(\Omega)$ *satisfying* $\int_\Omega \mathcal{A} \, d\mu \leq D_*$ *and obeying the constraints of* (3).

Corollary 1.3. *Under the assumptions of Proposition 1.2, one has* $D_* \geq d(s_*, s^*)$. *If equality holds, then the limit* μ *is a solution to* (3).

Interestingly, the proof of Proposition 1.2, presented §2.2, relies on a reinterpretation of the discretization (8) of Arnold's geodesic formulation (2) of Euler equations, which turns out to be the natural discretization of Brenier's relaxation (3) as well.

Figure 4: Illustration of Remark 1.6. The set S is the red curve and the set S_N is composed of the four large dots. The discretized geodesics is displayed as a dotted line. On the left, the penalization parameter λ is too small and the discretized geodesics takes "shortcuts", while on the right λ is too large, leading to overfitting.

Upper bounds on the discrete energy. Our main theorem establishes upper bounds on the discrete energies $\mathcal{E}(N, T, \lambda)$, for adequate values of the parameters, as required by the convergence result Proposition 1.2. It relies on a-priori assumptions on the structure of solutions to the continuous problem. The "relaxed" part of this result addresses the general case, based on Brenier's linear relaxation (3) of the Euler equations, and only requires on an assumption on the pressure regularity. The "classical" part provides a faster convergence rate under the assumption that Arnold's geodesic formulation (2) admits a minimizer $s : [0,1] \times X \to X$, of suitable regularity. At a given time t, the fluid velocity $\dot{s}(t,x)$ is uniquely determined by position $x \in X$ in the classical case, whereas in the relaxed case it is a probabilisitic superposition $\dot{\omega}(t)$ of velocities, weighted by the generalized flow solution $\mu \in \mathrm{Prob}(\Omega)$ conditional to $\omega(t) = x$; this is in a sense reminiscent of non-classical, quantum mechanics, hence the choice of adjective.

Recall that the classical (2) and relaxed (3) distances are automatically equal in dimension $d \geq 3$, and that the pressure field gradient ∇p is uniquely determined by the boundary values s_*, s^*.

Theorem 1.4. *Let $s_*, s^* \in \mathbb{S}$, let $T, N \in \mathbb{N}$, and $\lambda \geq 0$. The relaxed geodesic distance (3) and the discretized minimum (9) satisfy*

$$\mathcal{E}(T, N, \lambda) \leq d(s_*, s^*) + \mathcal{O}(Th_N^2 \lambda),$$

- *(Classical estimate) with $h_N = N^{-\frac{1}{d}}$ assuming that the classical geodesic distance (2) equals the relaxed distance (3), and admits a minimizer with regularity $s \in L^\infty([0,1], H^1(X))$.*

- *(Relaxed estimate) with $h_N = N^{-\frac{1}{2d}}$ (resp. $N^{-\frac{1}{2}}\sqrt{\ln N}$ if $d = 1$), if the pressure field gradient ∇p is Lipschitz on $[0,1] \times X$, and the boundary data s_*^{-1}, s^* are Lipschitz on X.*

Remark 1.5 (Optimal choice of the parameter λ). *Since the natural quantity occurring in the convergence analysis is $\mathcal{E}'(T, N, \lambda)$, see (12), it is natural to choose $\lambda = h_N^{-1} = N^{\frac{1}{D}}$ so that by Theorem 1.4*

$$\mathcal{E}'(T, N, \lambda) \leq d^2(s_*, s^*) + \mathcal{O}(T/\lambda + Th_N^2 \lambda) \leq d^2(s_*, s^*) + \mathcal{O}(TN^{-\frac{1}{D}}).$$

From this point, choosing $N, T \to \infty$ in such way that $TN^{-\frac{1}{D}} \to 0$, will fulfill the assumptions required by Proposition 1.2 for convergence.

Remark 1.6 (Finite-dimensional analogy for the choice of λ). *Consider a finite d-dimensional manifold S embedded in a Hilbert space M, whose minimising geodesics one wishes to approximate. The minimising geodesics between two points $s_*, s^* \in S$ can be approximated by minimisers of the energy*

$$(m_0, \ldots, m_T) \in M^{T+1} \mapsto T \sum_{0 \leq i < T} \|m_{i+1} - m_i\|^2 + \lambda \left(\|m_0 - s_*\| + \|m_T - s^*\| + \sum_{1 \leq i < T} d_{S_N}(m_i) \right),$$

8

where S_N is a sampling of the manifold S with N points. The choice of the optimal λ in term of convergence speed depends on the dimension of the manifold S and on the number of points N. Figure 4 illustrates that if λ is too small, the discrete geodesics takes "shortcuts", while if λ is too large it forms clusters around points in the discretization S_N. Note also that, for a fixed N and $\lambda \to \infty$, the optimization problem becomes combinatorial.

Establishing the upper bounds of Theorem 1.4 requires one to construct, for each choice of N, T, a candidate $m \in \mathbb{M}_N^{T+1}$ for the discrete problems (9) from a minimizer $\mu \in \mathrm{Prob}(\Omega)$ of the continuous problem (3). To do so, we approximate the probability measure μ by a measure μ_N uniformly supported over N paths. This amounts to solving a quantization problem [GG92] in the infinite-dimensional space Ω. Fortunately, the optimal speed of convergence of μ_N towards μ can be bounded in terms of the box dimension D of the support of μ (see Definition 4.1). This explains why the decay rate $h_N = N^{-\frac{1}{D}}$ in Theorem 1.4 depends, through the constant D, on the structure of the problem solution μ.

When the generalized flow μ is induced by a classical solution, as in (4), the particle trajectories are determined by their initial position $x \in X \subseteq \mathbb{R}^d$, so that μ is supported on a d-dimensional manifold, implying $D = d$. In the relaxed estimate however, the trajectories particles obey a second order ordinary differential equation (6) and are thus determined by their initial position and velocity $(x, v) \in X \times \mathbb{R}^d \subseteq \mathbb{R}^{2d}$ provided Picard-Lindelof/Cauchy-Lipschitz's theorem applies [CL55]. The quantization dimension of the generalized flow is thus $2d$ in the worst case, but intermediate dimensions $d < D < 2d$ are also common, see §5.

Outline. Propositions 1.1 and 1.2 are proved in §2. Theorem 1.4 is established in §3 (Classical estimate) and in §4 (Relaxed estimate). Numerical experiments are presented §5.

Remark 1.7 (Monge-Ampere gravitation). *Some models of reconstruction of the early universe [Bre11] involve actions of a form closely related to our discrete energy functional (9), for the parameter value $\lambda = 2$:*

$$\int_0^1 \left(\frac{1}{2} \|\dot{m}(t)\|^2 + \inf_{s \in \mathbb{S}} \|m(t) - s\|^2 \right) dt.$$

2 Convergence analysis

We prove Proposition 1.1 in §2.1 and Proposition 1.2 in §2.2, on the length of chains of incompressible maps, and the convergence of generalized flows respectively.

2.1 Length of a chain of incompressible maps

The announced Proposition 1.1 immediately follows from Lemma 2.1 below. It relies on a the following identity, valid for any elements a, b of a Hilbert space, and any $\varepsilon > 0$:

$$(1 + \varepsilon)^{-1} \|a + b\|^2 \leq \|a\|^2 + \varepsilon^{-1} \|b\|^2. \tag{13}$$

Indeed subtracting the LHS to the RHS of (13) we obtain $(1 + \varepsilon)^{-1} \|\varepsilon^{\frac{1}{2}} a - \varepsilon^{-\frac{1}{2}} b\|^2 \geq 0$.

Lemma 2.1. *For any $T \in \mathbb{N}^*$, any penalization $\lambda > 0$, and any $(m, s) \in (\mathbb{M} \times \mathbb{S})^{T+1}$ one has*

$$T \sum_{0 \leq i < T} \|s_{i+1} - s_i\|^2 \leq (1 + 4T/\lambda) \left[T \sum_{0 \leq i < T} \|m_{i+1} - m_i\|^2 + \lambda \sum_{0 \leq i \leq T} \|m_i - s_i\|^2 \right]. \tag{14}$$

Proof. Let $0 \le i < T$. Choosing $a := s_{i+1} - s_i$, and $b := m_{i+1} - m_i - a$, we obtain

$$(1+\varepsilon)^{-1}\|m_{i+1} - m_i\|^2 \le \|s_{i+1} - s_i\|^2 + \varepsilon^{-1}\|(s_i - m_i) - (s_{i+1} - m_{i+1})\|^2$$
$$\le \|s_{i+1} - s_i\|^2 + 2\varepsilon^{-1}(\|s_i - m_i\|^2 + \|s_{i+1} - m_{i+1}\|^2).$$

Summing over $0 \le i < T$ yields

$$(1+\varepsilon)^{-1}\sum_{0 \le i < T}\|m_{i+1} - m_i\|^2 \le \sum_{0 \le i < T}\|s_{i+1} - s_i\|^2 + 2\varepsilon^{-1}\sum_{0 \le i \le T}\alpha_i\|s_i - m_i\|^2,$$

with $\alpha_0 = \alpha_T = 1$, $\alpha_i = 2$ otherwise. Choosing $\varepsilon = 4T/\lambda$ concludes the proof. $\qquad\square$

2.2 Convergence towards generalized solutions

This subsection is devoted to the proof of Proposition 1.2. The discrete optimization problem (9) is inspired by Arnold's formulation (2) of Euler equations as a minimizing geodesic problem over $\mathbb{S}$. Our first lemma shows that, in the equivalent form (24), it could as well be regarded as a discretization of Brenier's relaxation (3). The terms $W_2^2(e_t\#\mu_m, \mathrm{Leb})$, where $m \in \mathbb{M}_N^{T+1}$ and μ_m is the induced generalized flow, can indeed be regarded as penalizations of the relaxed incompressibility constraint $e_t\#\mu = \mathrm{Leb}$ in (3). The other term $W_2^2((e_0, e_1)\#\mu_m, (s_*, s^*)\#\mathrm{Leb})$ enforces the proximity between the two couplings $(e_0, e_1)\#\mu_m$ and $(s_*, s^*)\#\mathrm{Leb}$ on X^2 as required in (3).

Lemma 2.2. *Let $m = (m_i)_{i=0}^T \in \mathbb{M}_N^{T+1}$ and $\mu_m \in \mathrm{Prob}(\omega)$ be the induced generalized flow. Then $\mathcal{E}(T, N, \lambda; m)$ equals*

$$\int_\Omega \mathcal{A}(\omega)d\mu_m(\omega) + \lambda\left(\int_X |m_0(x) - s_*(x)|^2 + |m_T(x) - s^*(x)|^2 dx + \sum_{\substack{1 \le i < T \\ t=i/T}} W_2^2(e_t\#\mu_m, \mathrm{Leb})\right). \quad (15)$$

In addition,

$$W_2^2((e_0, e_1)\#\mu_m, (s_*, s^*)\#\mathrm{Leb}) \le \int_X |m_0(x) - s_*(x)|^2 + |m_T(x) - s^*(x)|^2 dx. \quad (16)$$

Proof. Mimicking (5) at the discrete level, we obtain

$$\int_\Omega \mathcal{A}(\omega)d\mu(\omega) = \frac{1}{N}\sum_{1 \le j \le N}\int_0^1 |\dot\omega_j(t)|^2 dt = \frac{T}{N}\sum_{\substack{0 \le i < T \\ 1 \le j \le N}}|m_{i+1}^j - m_i^j|^2 = T\sum_{0 \le i < T}\|m_{i+1} - m_i\|^2,$$

On the other hand, Brenier's polar factorization theorem (10) yields $W_2^2(e_t\#\mu_m, \mathrm{Leb}) = d_\mathbb{S}^2(m)$, which gives (24).

The Wasserstein distance from $(e_0, e_1)\#\mu_m = (m_0, m_1)\#\mathrm{Leb}$ to $(s_*, s^*)\#\mathrm{Leb}$ appears on the LHS of (16). By definition, it is indeed bounded by the cost, appearing on the RHS, of the explicit transport plan $\pi = ((m_0, m_T), (s_*, s_*))\#\mathrm{Leb} \in \mathrm{Prob}(X^2 \times X^2)$, which sends $(m_0(x), m_T(x)) \mapsto (s_*(x), s^*(x))$ for all $x \in X$. $\qquad\square$

Our next step is to estimate the average violation of incompressibility by the discrete solution.

Lemma 2.3. *Let μ_m be the generalized flow associated to some $m \in \mathbb{M}_N^{T+1}$. Then*

$$\int_0^1 W_2^2(e_t\#\mu_m, \mathrm{Leb})\, dt \le \frac{1}{4T^2}\mathcal{E}'(T, N, \lambda; m).$$

10

Proof. Let $t \in [0,1]$, which we write $t = (i+\alpha)/T$ with $0 \le i < T$, $0 \le \alpha \le 1$. Then using (13) we obtain for any $\varepsilon > 0$,

$$W_2^2(\mathrm{e}_t \# \mu_m, \mathrm{Leb}) = \inf_{s \in \mathbb{S}} \|(1-\alpha)m_i + \alpha m_{i+1} - s\|^2 \le (1+\varepsilon)\left(\|\alpha(m_{i+1}-m_i)\|^2 + \varepsilon^{-1}\inf_{s \in \mathbb{S}}\|m_i - s\|^2\right)$$

Integrating over $t \in [0,1]$, and using that either $\alpha \le 1/2$ or $1-\alpha \le 1/2$, we obtain

$$\int_0^1 W_2^2(\mathrm{e}_t \# \mu, \mathrm{Leb})dt \le \frac{1+\varepsilon}{T}\sum_{0 \le i < T}\left(\frac{1}{4}\|m_{i+1}-m_i\|^2 + \varepsilon^{-1}\inf_{s \in \mathbb{S}}\|m_i - s\|^2\right)$$

which is precisely the announced estimate when $\varepsilon = 4T/\lambda$. $\qquad\square$

The convergence announced in Proposition 1.2, finally results from general compactness and continuity arguments.

Proof of Proposition 1.2. Let $T_k, N_k, \lambda_k, m_k, \mu_k$ and D_* be as in the statement of Proposition 1.2. The sublevel sets of the action, such as for any $\varepsilon > 0$

$$\{\mu \in \mathrm{Prob}(\Omega); \int_\Omega \mathcal{A}(\omega)d\mu(\omega) \le D_* + \varepsilon\}.$$

are weak-* sequentially compact by [Bre93]. Taking a subsequence if necessary, we assume that (μ_k) converges towards a $\mu_* \in \mathrm{Prob}(\Omega)$, which thus satisfies $\int_\Omega \mathcal{A}\,d\mu_* \le D_* + \varepsilon$ for any $\varepsilon > 0$, hence $\int_\Omega \mathcal{A}\,d\mu_* \le D_*$ as announced.

The functional $F : \mu \mapsto W_2^2((\mathrm{e}_0, \mathrm{e}_1)\#\mu, (s_*, s^*)\#\mathrm{Leb})$ is weak-* continuous on $\mathrm{Prob}(\Omega)$. By (16) one has $F(\mu_k) \le \frac{1}{\lambda_k}\mathcal{E}(T_k, N_k, \lambda_k; m_k) \to 0$ as $k \to \infty$, hence $F(\mu_*) = 0$ which implies

$$(\mathrm{e}_0, \mathrm{e}_1)\#\mu_* = (s_*, s^*)\#\mathrm{Leb}\,.$$

Similarly, the functional $G : \mu \mapsto \int_0^1 W_2^2(\mathrm{e}_t \# \mu, \mathrm{Leb})\,dt$ is weak-* lower semi-continuous on $\mathrm{Prob}(\Omega)$, as follows from Fatou's lemma and the continuity of $\mu \mapsto W_2^2(\mathrm{e}_t \# \mu, \mathrm{Leb})$ for any $t \in [0,1]$. By Lemma 2.3 one has $G(\mu_k) \to 0$ as $k \to \infty$, hence $G(\mu_*) = 0$ and therefore the limit generalizered flow obeys the incompressibility constraints

$$\forall t \in [0,1], \ \mathrm{e}_t \# \mu = \mathrm{Leb}\,. \qquad\square$$

3 Classical estimate

We establish in this section the first part of our main result, Theorem 1.4. By assumption, we consider a minimizer s of the shortest path problem (2), and assume that it has regularity $s \in L^\infty([0,1], H^1(X))$. Let also T, N, λ be the discrete problem parameters.

Define $s_i := s(i/T)$ for all $0 \le i \le T$, and note that $s_0 = s_*$ and $s_T = s^*$. Let also $m_i := \mathbb{P}_N(s_i)$, for all $0 \le i \le T$, where $\mathbb{P}_N : \mathbb{M} \to \mathbb{M}_N$ denotes the orthogonal projection. This construction is illustrated on Figure 5. The proof, short and elementary, proceeds by estimating the distance from m_i to s_i and to m_{i+1}, and then summing over the index $0 \le i \le T$.
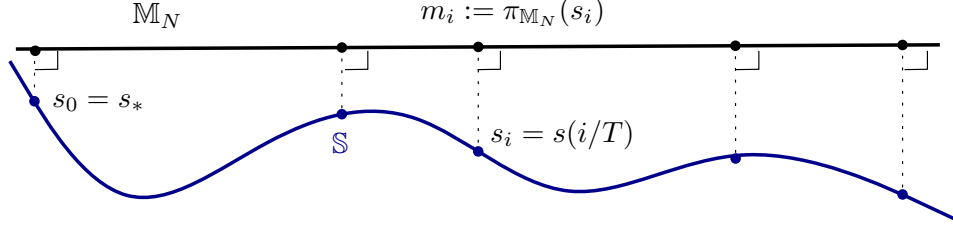
11

Figure 5: The classical estimate in Theorem 1.4 is based on projecting the measure preserving maps $(s_i)_{i=0}^T \in \mathbb{S}^{T+1}$ onto the finite dimensional space $\mathbb{M}_N$. This procedure is symmetrical to the projection of $(m_i)_{i=1}^{T-1} \in \mathbb{M}_N^{T-1}$ onto $\mathbb{S}$ involved in the discrete energy optimization (9), see Figure 2.

Distance from m_i to the set of incompressible maps. Denote by $h_N := N^{-\frac{1}{d}}$ the discretization scale, and recall that each region of the partition $\mathcal{P}_N$ of X has area $1/N$ and diameter $\leq C_{\mathcal{P}} h_N$. Let s_i^P denote the mean of s_i on the region P of the partition $\mathcal{P}_N$, for all $0 \leq i \leq T$. Then

$$\|s_i - m_i\|^2 = \sum_{P \in \mathcal{P}_N} \int_P |s_i(x) - s_i^P|^2 dx \leq C_{\mathrm{sb}}(C_{\mathcal{P}} h_N)^2 \sum_{P \in \mathcal{P}_N} \int_P |\nabla s_i(x)|^2 dx = C h_N^2 \|\nabla s_i\|^2,$$
(17)

where the Sobolev inequality constant C_{sb} only depends on the dimension, and $C := C_{\mathrm{sb}} C_{\mathcal{P}}^2$.

Distance from m_i to m_{i+1}. The map $\mathbb{P}_N$ is 1-Lipschitz, as it is the orthogonal projection onto the linear subspace $\mathbb{M}_N$. Hence for any $0 \leq i < T$

$$\|m_i - m_{i+1}\|^2 \leq \|s_i - s_{i+1}\|^2 \leq \frac{1}{T} \int_{\frac{i}{T}}^{\frac{i+1}{T}} \|\dot{s}(t)\|^2 dt.$$
(18)

Summation and conclusion. Summing (17) and (18) over $0 \leq i \leq T$ we obtain

$$\mathcal{E}(T, N, \lambda; m) \leq T \sum_{0 \leq i < T} \|m_{i+1} - m_i\|^2 + \lambda \sum_{0 \leq i \leq T} \|m_i - s_i\|^2$$

$$\leq \sum_{0 \leq i < T} \int_{\frac{i}{T}}^{\frac{i+1}{T}} \|\dot{s}(t)\|^2 dt + \lambda \sum_{0 \leq i \leq T} C h_N^2 \|\nabla s_i\|^2$$

$$\leq d^2(s_*, s^*) + C' T h_N^2 \lambda,$$

where $C' = C\|s\|_{L^\infty([0,1], H^1(X))}$, which concludes the proof.

4 Relaxed estimate

We prove the relaxed estimate in Theorem 1.4 using a quantization of the generalized flow minimizing the relaxed geodesic distance (3), in other words we approximate the solution $\mu \in \mathrm{Prob}(\Omega)$ with probability measures $(\mu_N)_{N \geq 1}$ equidistributed on a family of N paths. This quantization is a counterpart of the partition $\mathcal{P}_N$ of the domain (X, Leb) used for the classical estimate §3, which amounts to quantize the initial positions of the fluid particles.
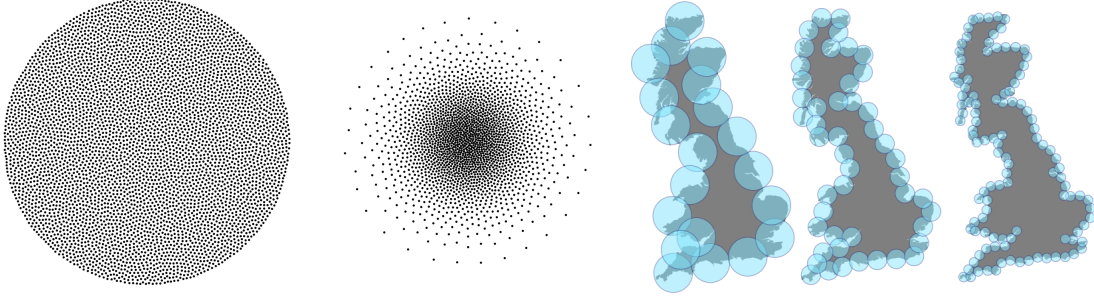
Figure 6: Left: Illustration of measure quantization. Two absolutely continuous probability measures over the disk (with constant density and a truncated Gaussian density) are approximated by finite collections of Dirac masses (shown as black dots) using the algorithm of De Goes et al [dGBOD12]. Right: Covering of the coast of England with N balls of minimal radius, as in (19). Image by A. Monnerot-Dumaine, source Wikipedia.

The proof is split into four parts. In §4.1, we introduce the framework of measure quantization. In §4.2, we specialize it to the case of Brenier's generalized flows. In §4.3 we perform a permutation of the obtained quantization, so as to match the boundary conditions. The announced energy estimate is finally proved in §4.4.

4.1 Box and quantization dimensions

In sampling theory, a natural objective is to approximate a given measure with a finite sum of Dirac masses in the Wasserstein distance, or to approximate a given set with a finite point set in the Haussdorff distance, see Figure 6. The quantization dimension of a measure, and the box dimension of a set, are defined as the optimal convergence rates of these approximation procedures.

We denote by δ_x the Dirac probability measure concentrated at a point x. The Haussdorff distance between two closed non-empty subsets A, B of a metric space is defined by

$$\text{Hauss}(A, B) := \max \left\{ \sup_{a \in A} d_B(a), \ \sup_{b \in B} d_A(b) \right\}, \qquad \text{where } d_Y(x) := \inf_{y \in Y} d(x, y).$$

Definition 4.1. *Let $\mathbb{H}$ be a metric space, let μ be a probability measure on $\mathbb{H}$, and let $\Gamma \subseteq \mathbb{H}$ be closed and non-empty. For all $N \geq 1$ denote*

$$h_N(\mu) := \inf_{\omega \in \mathbb{H}^N} W_2 \left(\mu, \ \frac{1}{N} \sum_{1 \leq i \leq N} \delta_{\omega_i} \right), \qquad r_N(\Gamma) := \inf_{\omega \in \mathbb{H}^N} \text{Hauss} \left(\Gamma, \ \{\omega_i\}_{i=1}^N \right).$$

The quantization dimension of μ, and the (upper) box dimension of Γ, are defined by

$$D_{\text{quant}}(\mu) := \limsup_{N \to \infty} \frac{\ln N}{-\ln h_N(\mu)}, \qquad D_{\text{box}}(\Gamma) := \limsup_{N \to \infty} \frac{\ln N}{-\ln r_N(\Gamma)}.$$

The box dimension D_{box} of a set — also called the Minkowski dimension — is a variant of the Haussdorff dimension in which the set of interest if covered with balls of *identical* radius. Indeed, one easily shows that $r_N(\Gamma)$ is the minimal radius allowing to cover Γ with N balls

$$r_N(\Gamma) := \inf_{\omega \in \mathbb{H}^N} \min \left\{ r \geq 0; \ \Gamma \subseteq \bigcup_{1 \leq i \leq N} \overline{B}(\omega_i, r) \right\}. \tag{19}$$

Box and Haussdorff dimension coincide for compact manifolds, but differ in general. For instance, all countable sets have Haussdorff dimension zero, whereas one can check that

$$D_{\text{box}}\left(([0,1]\cap\mathbb{Q})^d\right) = d, \qquad\qquad D_{\text{box}}\left(\left\{\frac{1}{n};\, n\in\mathbb{N}^*\right\}\right) = \frac{1}{2}.$$

The quantization dimension of a measure is bounded above by the box dimension of its support, as shows the following elementary result of quantization theory. We refer the reader to [GG92] for more details on this rich subject.

Proposition 4.2. *Let $\mathbb{H}$ be a metric space, and let $\mu\in\text{Prob}(\mathbb{H})$ be supported on a set Γ. Then $D_{\text{quant}}(\mu) \leq \max\{2, D_{\text{box}}(\Gamma)\}$. More precisely for any $D > 0$, one has as $N\to\infty$*

$$r_N(\Gamma) = \mathcal{O}(N^{-\frac{1}{D}}) \quad\Rightarrow\quad h_N(\mu) = \mathcal{O}\begin{cases} N^{-\frac{1}{D}} & \text{if } D > 2, \\ N^{-\frac{1}{2}}\sqrt{\ln N} & \text{if } D = 2, \\ N^{-\frac{1}{2}} & \text{if } D < 2. \end{cases} \tag{20}$$

Proof. Let $N\in\mathbb{N}$ be fixed. For each $1\leq i\leq N$ let $M_i\subseteq\mathbb{H}$ be a set of i points such that $\Gamma\subseteq\cup_{\omega\in M_i}\overline{B}(\omega, 2r_i)$, with $r_i := r_i(\Gamma)$. We construct a sequence of points $\omega_i\in\mathbb{H}$, and an increasing sequence of measures ρ_i supported on Γ and of mass i/N, inductively starting with $i = N$ and finishing with $i = 1$. Initialization: $\rho_N := \mu$.

Induction: for each $1\leq i\leq N$, we construct ω_i and ρ_{i-1} in terms of ρ_i. Let indeed $\omega_i\in M_i$ be such that $B_i := \overline{B}(\omega_i, 2r_i)$ satisfies $\rho_i(B_i)\geq 1/N$. Such a point exists since $|\rho_i| = i/N$, $\#(M_i) = i$, and $\text{supp}(\rho_i)\subseteq\Gamma$. Then let $\rho_{i-1} := \rho_i - \frac{1}{N\rho_i(B_i)}\rho_i$, so that $\rho_i - \rho_{i-1}$ is a non-negative measure of mass $\frac{1}{N}$ supported on $\overline{B}_i$. One has

$$h_N(\mu)^2 \leq W_2^2\left(\mu, \frac{1}{N}\sum_{1\leq i\leq N}\delta_{\omega_i}\right) \leq \sum_{1\leq i\leq N}W_2^2\left(\rho_i - \rho_{i-1}, \frac{1}{N}\delta_{\omega_i}\right) \leq \frac{1}{N}\sum_{1\leq i\leq N}(2r_i)^2.$$

The comparison (20) of the decay rates of $h_N(\mu)$ and $r_N(\Gamma)$ immediately follows. Finally the comparison of the dimensions follows from (20). $\qquad\square$

4.2 Quantization dimension of a generalized flow

We specialize in this subsection the measure μ, support Γ and embedding metric space $\mathbb{H}$ to which we apply the results of §4.1. Let $\mu\in\text{Prob}(\Omega)$ be a generalized flow minimizing the relaxed geodesic distance (3). This measure is concentrated on the set Γ of paths obeying Newton's second law of motion

$$\Gamma := \{\omega\in C^2([0,1], X);\, \forall t\in[0,1],\, \ddot{\omega}(t) = -\nabla p(t, \omega(t))\}, \tag{21}$$

where the pressure gradient $\nabla p : [0,1]\times X\to\mathbb{R}^d$ is assumed to have Lipschitz regularity, following the assumptions of Theorem 1.4. We regard Γ as embedded in the Hilbert space $\mathbb{H} := H^1([0,1], \mathbb{R}^d)$, which plays a natural role in the problem of interest (3) and is equipped with the norm

$$\|\omega\|_{\mathbb{H}}^2 := \int_0^1 |\omega|^2 + |\dot{\omega}|^2.$$

Note that $\mathbb{H}$ continuously embeds in $C^0([0,1], \mathbb{R}^d)$, hence the evaluation maps $e_t : \mathbb{H}\to\mathbb{R}^d : \omega\mapsto \omega(t)$ are continuous with a common Lipschitz constant denoted C_e.

Notation 4.3 (Problem constants). *The following quantities are referred to as the* problem constants: *the dimension d, the constant $C_{\mathcal{P}}$ related to the partitions, the Lipschitz regularity constants C_* and C^* of the boundary conditions s_*^{-1} and s^*, the maximum norm and the Lipschitz regularity regularity constant of the pressure gradient ∇p. Given two expressions A, B, we write $A \lesssim B$ iff $A \leq CB$ for some constant C that only depends on the problem constants.*

Using a general existence and stability result for ODEs, Lemma 4.4, we show that Γ is in bijection with a compact subset of $\mathbb{R}^{2d}$, in Lemma 4.5.

Lemma 4.4. *Let $F \in C^0([0,1] \times \mathbb{R}^n, \mathbb{R}^n)$ be Lipscshitz in the second variable, uniformly with respect to the first variable: $\exists L, \forall t \in [0,1], \forall y_1, y_2 \in \mathbb{R}^n, |F(t, y_1) - F(t, y_2)| \leq L|y_1 - y_2|$. Then the map $\mathbb{R}^n \to L^2([0,1], \mathbb{R}^n)$, associating to each $y_0 \in \mathbb{R}^n$ the solution to the ODE $y'(t) = F(t, y(t))$ with initial condition $y(0) = y_0$, is bi-Lipschitz onto its image with regularity constant e^L.*

Proof. The Picard-Lindelof/Cauchy-Lipschitz Theorem [CL55] guarantees the existence of a unique solution to the considered ODE. If y_1, y_2 are two such solutions, then for any $t \in [0,1]$

$$|\dot{y}_1(t) - \dot{y}_2(t)| = |F(t, y_1(t)) - F(t, y_2(t))| \leq L|y_1(t) - y_2(t)|$$

Thus for any $t \in [0,1]$

$$e^{-Lt}|y_1(0) - y_2(0)| \leq |y_1(t) - y_2(t)| \leq e^{Lt}|y_1(0) - y_2(0)|,$$

hence by integration over $t \in [0,1]$, as announced

$$e^{-L}|y_1(0) - y_2(0)| \leq \|y_1 - y_2\|_{L^2([0,1])} \leq e^L|y_1(0) - y_2(0)|. \qquad \square$$

The image of the generalized flow μ by the map of initial position and momentum, used in the next lemma, is often called a minimal measure [BFS09].

Lemma 4.5. *The map $E_0 : \Gamma \to X \times \mathbb{R}^d : \omega \mapsto (\omega(0), \dot{\omega}(0))$ is bijective and bi-Lipschitz onto its image, which is a compact set. The Lipschitz régularity constants, and the image diameter, can be bounded in terms of the problem constants, see Notation 4.3.*

Proof. The function $F(t, x, v) := (v, -\nabla p(t, x))$ is Lipschitz on $[0,1] \times X \times \mathbb{R}^d$, with a regularity constant determined by that of ∇p. It can be extended to $[0,1] \times \mathbb{R}^{2d}$. Applying Lemma 4.4 to F in dimension $n = 2d$, we obtain as announced that E_0 is bi-Lipschitz onto its image. Note that the norm $\|(\omega, \dot{\omega})\|_{L^2([0,1])}$ appearing in this estimate is precisely $\|\omega\|_{\mathbb{H}}$.

By construction, $\omega(t)$ and $\ddot{\omega}(t)$ are uniformly bounded for all $\omega \in \Gamma$, and all $t \in [0]$, respectively by the diameter of X and the maximum norm of ∇p. This implies an upper bound on $\dot{\omega}(0)$, observing for instance that

$$|\omega(0) - \omega(1)| = \left|\int_0^1 \dot{\omega}(t)\,dt\right| \geq |\dot{\omega}(0)| - \int_0^1 |\dot{\omega}(t) - \dot{\omega}(0)|dt \geq |\omega(0)| - \int_0^1 |\ddot{\omega}(t)|dt.$$

As announced, the image of Γ by E_0 is bounded, hence compact since it is clearly closed. $\qquad \square$

Since there is no ambiguity, we denote in the rest of this section $h_N := h_N(\mu)$. The information gathered on the set Γ supporting μ yields upper and lower bounds on the decay rate of (h_N), obtained respectively in Corollary 4.6 and Proposition 4.7.

Corollary 4.6. *One has $h_N \lesssim N^{-\frac{1}{2d}}$ (resp. $h_N \lesssim N^{-\frac{1}{2}}\sqrt{\ln N}$ if $d = 1$) for all $N \geq 2$.*

Proof. By Lemma 4.5, the set Γ is in bi-Lipschitz bijection with a compact set $K \subseteq \mathbb{R}^{2d}$. Hence $r_N(\Gamma) \lesssim r_N(K) \lesssim N^{-\frac{1}{2d}}$, and the upper estimate follows from (20). $\qquad\square$

The quantization scale h_N is also bounded below, and is minimal for classical solutions.

Proposition 4.7. *One has $h_N \gtrsim N^{-\frac{1}{d}}$ for all $N \geq 1$. If the generalized flow μ in fact represents a classical solution s to Euler's equations, and $\nabla \dot{s}$ is bounded on $[0,1] \times X$, then this lower estimate is sharp: $h_N \lesssim N^{-\frac{1}{d}}$.*

Proof. Since X is a domain of unit area, there exists $c > 0$ depending only on the dimension d and such that $W_2(\mathrm{Leb}, \nu_N) \geq cN^{-\frac{1}{d}}$ for any measure ν_N supported at N points of $\mathbb{R}^d$. The first point follows: for any measure μ_N supported at N points of $\mathbb{H}$

$$ cN^{-\frac{1}{d}} \leq W_2(\mathrm{Leb}, \mathrm{e}_0 \# \mu_N) = W_2(\mathrm{e}_0 \# \mu, \mathrm{e}_0 \# \mu_N) \leq C_{\mathrm{e}} W_2(\mu, \mu_N) = C_{\mathrm{e}} h_N. $$

Second point: for each $x \in X$, introduce the path $\omega_x : [0,1] \to \mathbb{R}^d : t \mapsto s(t, x)$. Then $\Phi : (X, \mathrm{Leb}) \to (\Gamma, \mu) : x \mapsto \omega_x$ is measure preserving and Lipschitz, with regularity constant denoted C_Φ (which we regard as a problem constant). Let ν_N be a discrete probability measure, with one Dirac mass of weight $1/N$ in each region of the partition $\mathcal{P}_N$. Since these regions have diameter $\leq C_{\mathcal{P}} N^{-\frac{1}{d}}$, we conclude that

$$ h_N \leq W_2(\mu, \Phi \# \nu_N) = W_2(\Phi \# \mathrm{Leb}, \Phi \# \nu_N) \leq C_\Phi W_2(\mathrm{Leb}, \nu_N) \leq C_\Phi C_{\mathcal{P}} N^{-\frac{1}{d}}. \qquad\square $$

4.3 Permutation of the quantization of μ and boundary conditions

We have shown §4.2 that the generalized flow, solution to Brenier's relaxation of Euler's equations (3), could be approximated (quantized) by a finite family of particle paths, with a controlled convergence rate. This is not yet sufficient however to construct a good candidate for the discrete energy (8), despite its relaxed reformulation (24). For that purpose one needs to permute the paths, so as to match the boundary conditions, as required by the energy term (16).

We show in Lemma 4.8 that an optimal quantization exists, we suitably permute it in Lemma 4.9 and estimate a first boundary term, and we estimate the second boundary term in Proposition 4.10. In this subsection and the next, we fix the integer N and allow ourselves a slight abuse of notation: elements $\omega_j, P_j, \rho_j, \dots$ indexed by $1 \leq j \leq N$ do implicitly depend on N, although that second index $\omega_j^N, P_j^N, \rho_j^N, \dots$ is omitted for readability.

Lemma 4.8. *The infimum defining h_N is attained, see Definition 4.1. As a result there exists $(\omega_j)_{j=1}^N \in \mathbb{H}^N$ and probability measures $(\rho_j)_{j=1}^N$ on Γ such that*

$$ \mu = \frac{1}{N} \sum_{1 \leq j \leq N} \rho_j \qquad\qquad h_N^2 = \frac{1}{N} \sum_{1 \leq j \leq N} \int_\Gamma \|\omega - \omega_j\|_{\mathbb{H}}^2 \, d\rho_j(\omega) \qquad (22) $$

Furthermore, ω_j is the barycenter of ρ_j for each $1 \leq j \leq N$.

Proof. Let $(\omega_j)_{j=1}^N$ be a candidate quantization, and let π be the transport plan associated to $W_2^2(\frac{1}{N} \sum_{j=1}^N \delta_{\omega_j}, \mu)$. Then the measures $\rho_j : A \mapsto N\pi(\{\omega_j\} \times A)$, $1 \leq j \leq N$, are probabilities which average to μ, and the transport cost is the RHS of (22). The quantization energy, i.e. the squared Wasserstein distance, is decreased when replacing ω_j with the barycenter b_j of ρ_j, $1 \leq j \leq N$, by the amount $\frac{1}{N} \sum_{j=1}^N |\omega_j - b_i|^2$. Hence $\omega_j = b_j$ for all $1 \leq j \leq N$ if the quantization is optimal. Note also that the barycenter of ρ_j belongs to $G := \overline{\mathrm{Hull}(\Gamma)}$ by construction.

Since Γ is a compact subset of a Hilbert space, the convex hull closure G is also compact, for the strong topology induced by $\|\cdot\|_{\mathbb{H}}$. The quantization energy $(\omega_j)_{j=1}^N \mapsto W_2^2(\frac{1}{N}\sum_{j=1}^N \delta_{\omega_j}, \mu)$ attains its minimum on G^N by compactness, and by the previous argument it is the global minimum on $\mathbb{H}^N$. $\qquad\square$

Let μ_N denote the equidistributed probability on the set $\{\omega_j;\ 1 \le j \le N\}$ of Lemma 4.8.

Lemma 4.9. *The paths $(\omega_j)_{j=1}^N$ of the quantization μ_N, and the regions $(P_j)_{j=1}^N$ of the partition $\mathcal{P}_N$, can be indexed in such way that*

$$\sum_{1 \le j \le N} \int_{P_j} |\omega_j(0) - s_*(x)|^2 dx \lesssim h_N^2. \qquad (23)$$

Proof. Let $(P_j)_{j=1}^N$ be an arbitrary indexation of $\mathcal{P}_N$. Let a_j be the barycenter of region P_j, and b_j the barycenter of the image region $s_*(b_j)$. For any $1 \le j \le N$ one has by assumption

$$\int_{P_j} |b_j - s_*(x)|^2 dx \le \int_{P_j} |s_*(a_j) - s_*(x)|^2 dx \le C_*^2 \int_{P_j} |a_j - x|^2 dx \le \frac{1}{N}(C_* C_{\mathcal{P}} N^{-\frac{1}{d}})^2,$$

where C_* denotes the Lipschitz regularity constant of s_*^{-1}. Denoting by ν_N the discrete measure equidistributed at the N points $(b_j)_{j=1}^N$, we obtain

$$W_2(\nu_N, \text{Leb}) \le \sqrt{\sum_{1 \le j \le N} \int_{P_j} |b_j - s_*(x)|^2 dx} \lesssim N^{-\frac{1}{d}}.$$

On the other hand $W_2(\text{Leb}, e_0 \# \mu_N) \le C_e W_2(\mu, \mu_N) = C_e h_N$. Thus $W_2(\nu_N, e_0 \# \mu_N) \lesssim h_N$, since W_2 defines a distance, and since $h_N \gtrsim N^{-\frac{1}{d}}$ by Proposition 4.7. This optimal transport problem between the discrete measures ν_N and $e_0 \# \mu_N$ determines an optimal assignment $\Gamma_N \to B_N$. Up to a permutation of the paths $(\omega_j)_{j=1}^N$, we assume that this assignment is represented by the common indexation $(\omega_j)_{j=1}^N$ of Γ_N and $(b_j)_{j=1}^N$ of B_N. Finally

$$\sum_{1 \le j \le N} \int_{P_j} |\omega_j(0) - s_*(x)|^2 dx = \sum_{1 \le j \le N} \int_{P_j} |b_j - s_*(x)|^2 dx + W_2^2(\nu_N, e_0 \# \mu_N) \lesssim h_N^2. \qquad \square$$

Proposition 4.10. *Using the indexation of Lemma 4.9, one has*

$$\sum_{1 \le j \le N} \int_{P_j} |\omega_j(1) - s^*(x)|^2 dx \le C h_N^2.$$

Proof. The generalized boundary condition of (3) states that $\omega(1) = s_*^*(\omega(0))$ for μ-almost every $\omega \in \Gamma$, where $s_*^* := s^* \circ s_*^{-1}$. Denoting by C_*^* the Lipschitz regularity constant of s_*^*, we obtain for any $1 \le j \le N$ and any $x \in X$

$$|\omega_j(1) - s^*(x)|^2 = \left| \int_\Gamma s_*^*(\omega(0)) - s^*(x)\, d\rho_j(\omega) \right|^2 \le \int_\Gamma |s_*^*(\omega(0)) - s^*(x)|^2\, d\rho_j(\omega)$$

$$\le (C_*^*)^2 \int_\Gamma |\omega(0) - s_*(x)|^2\, d\rho_j(\omega) \le 2(C_*^*)^2 \left(\int_\Gamma |\omega(0) - \omega_j(0)|^2\, d\rho_j(\omega) + |\omega_j(0) - s_*(x)|^2 \right).$$

By summation and integration we conclude, using Lemma 4.9 in the second line,

$$\sum_{1 \le j \le N} \int_{P_j} |\omega_j(1) - s^*(x)|^2\, dx \lesssim \sum_{1 \le j \le N} \frac{1}{N} \int_\Gamma |\omega_j(0) - \omega(0)|^2\, d\rho_j(\omega) + \sum_{1 \le j \le N} \int_{P_j} |\omega_j(0) - s_*(x)|^2\, dx$$

$$\le C_e^2 W_2^2(\mu_N, \mu) + C h_N^2 \lesssim h_N^2. \qquad \square$$

4.4 Final estimate

We conclude in this subsection the proof of Theorem 1.4 (Relaxed estimate). Let $\mu \in \mathrm{Prob}(\Omega)$ be a generalized flow minimizing (3), with an associated Lipschitz pressure gradient. We fix the parameters (T, N), and consider an optimal quantization μ_N supported on N paths $(\omega_j)_{j=1}^N$ as in Lemma 4.8. For each $0 \leq i \leq T$, let $m_i \in \mathbb{N}$ be the piecewise constant map on the partition $\mathcal{P}_N$ defined by

$$\forall 1 \leq j \leq N, \ \forall x \in P_j, \ m_i(x) := \omega_j(i/T).$$

In the following, we bound each of the terms of the energy $\mathcal{E}(T, N, \lambda; m) \geq \mathcal{E}(T, N, \lambda)$. By Lemma 4.9 and Proposition 1.2, one has respectively

$$\|m_0 - s_*\|^2 \lesssim h_N^2, \qquad\qquad \|m_T - s^*\|^2 \lesssim h_N^2.$$

Regarding the distance to incompressible maps, one has for any $1 \leq i < T$, with $t := i/T$

$$\inf_{s \in \mathbb{S}} \|m_i - s\| = W_2(\mathrm{Leb}, \mathrm{e}_t \# \mu_N) = W_2(\mathrm{e}_t \# \mu, \mathrm{e}_t \# \mu_N) \leq C_e W_2(\mu, \mu_N) = C_e h_N.$$

We use the Cauchy-Schwartz inequality to bound the action:

$$T \sum_{0 \leq i < T} \|m_{i+1} - m_i\|^2 = \frac{1}{N} \sum_{1 \leq j \leq N} T \sum_{0 \leq i < T} \left| \omega_j\left(\frac{i+1}{T}\right) - \omega_j\left(\frac{i}{T}\right) \right|^2 \leq \frac{1}{N} \sum_{1 \leq j \leq N} \int_0^1 |\dot\omega_j(t)|^2 dt$$

$$= \frac{1}{N} \sum_{1 \leq j \leq N} \int_0^1 \left| \int_\Gamma \dot\omega \, d\rho_j(\omega) \right|^2 \leq \frac{1}{N} \sum_{1 \leq j \leq N} \int_0^1 \int_\Gamma |\dot\omega|^2 \, d\rho_j(\omega) \, dt = d^2(s_*, s^*).$$

Concluding, the value $\mathcal{E}(T, N, \lambda)$ is bounded by

$$T \sum_{0 \leq i < T} \|m_{i+1} - m_i\|^2 + \lambda \left(\|m_0 - s_*\|^2 + \|m_T - s^*\|^2 + \sum_{1 \leq i < T} \inf_{s \in \mathbb{S}} \|m_i - s\|^2 \right) \leq d^2(s_*, s^*) + \mathcal{O}(T h_N^2 \lambda).$$

5 Numerical experiments

5.1 Minimization algorithm and choice of penalization

We rely on a quasi-Newton method to compute a (local) minimum of the discretized problem (9), as summarized in Algorithm 1. This means that we need to compute the value of the functional

$$m \in \mathbb{M}_N^{T+1} \mapsto T \sum_{0 \leq i < T} \|m_{i+1} - m_i\|^2 + \lambda \left(\|m_0 - s_*\|^2 + \|m_T - s^*\|^2 + \sum_{1 \leq i < T} d_{\mathbb{S}}^2(m_i) \right). \quad (24)$$

and its gradient, where $d_{\mathbb{S}}^2(m) = \inf_{s \in \mathbb{S}} \|m - s\|^2$. The only difficulty is to evaluate the squared distance $d_{\mathbb{S}}^2$ to the set of measure-preserving vector fields and its gradient. As explained in the introduction, Brenier's Polar Factorization Theorem implies that for any vector-valued function $m \in \mathbb{M}$,

$$d_{\mathbb{S}}^2(m) = W_2^2(m\# \mathrm{Leb}, \mathrm{Leb}).$$

When m belongs to $\mathbb{M}_N$, the measure $m\# \mathrm{Leb}$ is finitely supported, and the computation of the Wasserstein distance can be performed using a solver for semi-discrete optimal transport, such as [AHA98, Mer11, dGBOD12, Lév14]. The next proposition gives an explicit formulation for the gradient in term of the optimal transport plan. Note that the expression of the gradient of

the semi-discrete Kantorovitch functional with respect to the position of the points also appears in the appendix of [dGBOD12].

Recall that $\mathbb{M}_N$ is the set of piecewise constant functions on the tessellation $\mathcal{P}_N := (P_j)_{1 \leq j \leq N}$ of X. The diagonal $\mathbb{D}_N$ in $\mathbb{M}_N$ is the set of functions m in $\mathbb{M}_N$ such that $m(P_j) = m(P_k)$ for some $j \neq k$. The set $\mathbb{M}_N \setminus \mathbb{D}_N$ is a dense open set in $\mathbb{M}_N$.

Proposition 5.1. *The functional $d_{\mathbb{S}}^2$ is differentiable almost everywhere on $\mathbb{M}_N$ and continuously differentiable on $\mathbb{M}_N \setminus \mathbb{D}_N$. The gradient of $d_{\mathbb{S}}^2$ at $m \in \mathbb{M}_N \setminus \mathbb{D}_N$ is explicit: with $x_j = m(P_j)$,*

$$\nabla d_{\mathbb{S}}^2(m)\big|_{P_j} = 2(x_j - \mathrm{bary}(T^{-1}(x_j))) \tag{25}$$

where $T : X \to m(X)$ is the piecewise constant optimal transport map between Leb and the finitely supported measure $m\#\mathrm{Leb}$, and $\mathrm{bary}(S) = \int_S x\,dx / \mathrm{Leb}(S)$ is the isobarycenter of S

Proof. The functional $\mathcal{F} := d_{\mathbb{S}}^2 - \|\cdot\|^2$ is concave as an infimum of linear functions:

$$\mathcal{F}(m) = d_{\mathbb{S}}^2(m) - \|m\|^2 = \inf_{s \in \mathbb{S}} \|m - s\|^2 - \|m\|^2 = \inf_{s \in \mathbb{S}} \left[-2\langle m|s \rangle + \|s\|^2 \right],$$

where $\langle \cdot, \cdot \rangle$ denotes the $L^2(X)$ scalar product. This implies in particular that $\mathcal{F}$ and therefore $d_{\mathbb{S}}^2$ is differentiable almost everywhere on $\mathbb{M}_N$. Given m in $\mathbb{M}_N \setminus \mathbb{D}_N$, define $x_j = m(P_j)$ and let $T : X \to \mathbb{R}^d$ be the optimal transport plan from Leb to $m\#\mathrm{Leb} = \frac{1}{N} \sum_{j=1}^{N} \delta_{x_j}$. The transport plan is indeed always representable by a function when the source measure is absolutely continuous with respect to the Lebesgue measure. Let $V_j = T^{-1}(x_j)$ be the partition of X induced by this transport plan. Then

$$\mathcal{F}(m) = W_2^2(m\#\mathrm{Leb}, \mathrm{Leb}) - \|m\|^2 = \sum_{j=1}^{N} \int_{V_j} \|x_j - x\|^2 - \|x_j\|^2 dx$$

$$= \langle m|G(m) \rangle + \sum_{j=1}^{N} \int_{V_j} \|x\|^2 dx$$

where $G(m) \in \mathbb{M}_N$ is the piecewise constant function on X given by $G(m)|_{P_j} = -2\,\mathrm{bary}(V_j)$. For any m' in $\mathbb{M}_N$ and $x_j' = m'(V_j)$, one has

$$\mathcal{F}(m') = W_2^2(m'\#\mathrm{Leb}, \mathrm{Leb}) - \|m'\|^2 \leq \sum_{j=1}^{N} \int_{V_j} \|x_j' - x\|^2 - \|x_j'\|^2 dx$$

$$= \mathcal{F}(m) + \langle m' - m|G(m) \rangle$$

This shows that $G(m)$ belongs to the superdifferential to $\mathcal{F}$ at m. In addition, by the continuity of optimal transport plans, the map $m \in \mathbb{M}_N \setminus \mathbb{D}_N \mapsto G(m)$ is continuous. To summarize, on the open domain $\mathbb{M}_N \setminus \mathbb{D}_N$ the concave function $\mathcal{F}$ possesses a continuous selection of supergradient. This implies that $\mathcal{F}$ is of class $\mathcal{C}^1$ on this domain, with $\nabla F(m) = G$, and the result follows. $\quad\square$

Remark 5.2 (Computation of $d_{\mathbb{S}}^2$). *The computation of the squared distance to measure-preserving maps $d_{\mathbb{S}}^2$ and its gradient rely on the variational approach used in the proof of the above proposition. We use the CGAL library [cga] to evaluate $\mathcal{F}$ and its first and second derivatives, and a simple damped Newton's algorithm to compute its maximum. The implementation is available at https://github.com/mrgt/PyMongeAmpere.*

Construction of the initial solution Since the discrete energy (8) is non-convex, the construction of the inital guess is important. We follow a time-refinement strategy already used by Brenier [Bre08] to construct a good initial guess. Assuming that we have already a local minimizer for $T_k = 2^k + 1$, we use linear interpolation to construct an initial guess for $T_{k+1} = 2^{k+1} + 1$. The optimization is then performed from this inital guess, using a quasi-Newton algorithm for the energy (8).

Choice of the penalization parameter The optimal choice of λ in (8) depends on the quantization dimension $D = D_{\text{quant}}(\mu)$ of the generalized solution $\mu \in \text{Prob}(\Omega)$ that one expects to recover: namely $\lambda_N = N^{-\frac{1}{D}}$, see Remark 1.5. We call D the flow dimension, and regard it as as the intrinsic dimensionality of the problem which determines its computational difficulty. For a classical solution, this dimension agrees with the ambient dimension i.e. $D = d$, while for a non-deterministic solution the quantization dimension can be up to $2d$. Intermediate dimensions $d < D < 2d$ are also common [Bre89]. In our numerical experiments we set $\lambda_N = N^{\frac{1}{3}}$, a decision justified a-posteriori by the numerical estimation of the quantization dimension of the computed solution, see Figure 8.

Note that the numerical error in (1.5) is governed (for a fixed number T of time steps) by the quantity $\lambda^{-1} + h_N^2 \lambda$, and that $h_N = \mathcal{O}(N^{-\frac{1}{2d}})$ under the assumptions of Theorem 1.4. The choice $\lambda_N = N^{\frac{1}{\alpha}}$ thus yields a convergent scheme whenever $\alpha > d$, although convergence rates are improved if α is close to the flow dimension D, so that $\lambda_N \approx N^{\frac{1}{D}} \approx h_N^{-1}$.

Algorithm 1 Computation of a (local) minimizer for (24).

> **For** $k = 1 \ldots k_{\max}$
>> $T := 2^k$
>> for all even $t \in \{0, \ldots, T\}$, let $m_i^k := m_{i/2}^{k-1}$ *initialize discrete geodesic*
>> for all odd $t \in \{1, \ldots, T\}$, let $m_i^k := \frac{1}{2}(m_{i-1}^k + m_{i+1}^k)$
>> **Until convergence do**   *optimize*
>>> for all i, compute $d_{\mathbb{S}}(m_i)$ and $\nabla d_{\mathbb{S}}(m_i)$ *see Rem. 5.2*
>>> compute the discrete path energy and its gradient   *see Eq. (24)*
>>> update $(m_i^k)_{0 \leq t \leq T}$ using the L-BFGS scheme   *see [BLNZ95]*

5.2 Visualization of generalized solution

The main interest of numerical experimentation is to visualize generalized solutions to Euler's equation, or equivalently generalized geodesics between two measure-preserving diffeomorphisms s_*, s^* in $\mathbb{S}$.

5.2.1 Gradient of the pressure

Consider a minimizer of the discretized energy (8). Given $i \in \{1, \ldots, T-1\}$, m_i minimizes over $\mathbb{M}_N$ the functional $m \mapsto T(\|m - m_{i-1}\|^2 + \|m_{i+1} - m\|^2) + \lambda d_{\mathbb{S}}^2(m)$. This gives

$$T^2(m_{i-1} - 2m_i + m_{i+1}) = T\lambda \nabla d_{\mathbb{S}}^2(m_i). \tag{26}$$

This equation is a discretized counterpart of the rule that the acceleration of a geodesic on an embedded manifold, is normal to that manifold (here $\mathbb{S}$ plays the role of the manifold, embedded in $\mathbb{M}$, which is internally approximated by the linear space $\mathbb{M}_N$). The second order difference

$T^2(m_{i-1} - 2m_i + m_{i+1})$ approximates a second derivative in time. Comparing (26) to (6), we see that the right hand-side of (26) can be used as an estimation of (minus) the gradient of the pressure.

5.2.2 Geometric data analysis

As in the proof of Theorem 1.4, the discrete minimizer of (8) can converted to a collection of N piecewise-linear curves $\{\omega_1, \ldots, \omega_N\} = \Gamma_N$. We recall that the domain X is partitioned into N subdomains $(P_j)_{1 \leq j \leq N}$ with equal area and we let $\omega_j(i/T) \in \mathbb{R}^d$ be the point corresponding to the restriction of m_i to the subdomain P_j, for each $0 \leq i \leq T$. Figure 3 illustrates this construction. We regard Γ_N as embedded in the Hilbert space $\mathbb{H} := H^1([0,1], \mathbb{R}^2)$ which plays a natural role in the problem of interest, as in §4, and apply techniques from the field of geometric data analysis.

Clustering In order to better visualize the solution, we use the k-means algorithm to divide the set Γ_N into k. A distinct particle color is attached to each cluster, see for instance Figure 10. The k-means algorithm consists in finding a local minimizer of the optimal quantization problem

$$\min_{\ell_1, \ldots \ell_k \in \mathbb{H}} \frac{1}{N} \sum_{\omega \in \Gamma_N} \min_{1 \leq i \leq k} \|\omega - \ell_i\|_{\mathbb{H}}^2 \tag{27}$$

using a simple fixed point algorithm, and to divide Γ_N into clusters $(C_i)_{1 \leq i \leq k}$ with

$$C_i = \left\{ \omega \in \Gamma_N; \|\omega - \ell_i\|_{\mathbb{H}} = \arg \min_{1 \leq j \leq k} \|\omega - \ell_i\|_{\mathbb{H}} \right\}.$$

Note that $l_1, \cdots, l_k$ automatically belong to $\mathrm{Span}(\Gamma_N)$, hence to the $d(T+1)$-dimensional linear subspace of $\mathbb{H}$ consisting of piecewise linear paths with nodes $\omega(t) \in \mathbb{R}^d$ at times $t = i/T$, $0 \leq i \leq T$. This makes (27) tractable.

Let μ be the probability measure supported on the set $\Gamma_N \subseteq \mathbb{H}$, with weight $1/N$ for each element. The k-means problem amounts to finding the probability measure μ_k, supported on at most k points of $\mathbb{H}$, which is the closest to μ w.r.t. the Wasserstein distance: (27) equals

$$\min_{\#(\mathrm{supp}\,\mu_k) \leq k} W_2^2(\mu, \mu_k).$$

This quantization problem is closely related to the one defining $h_N(\mu)$ in Definition 4.1, up to the difference that the candidate measure μ_k need not be equidistributed on the k points of its support.

Box dimension A natural objective is to estimate the quantization dimension $D_{\mathrm{quant}}(\mu)$ of the generalized flow $\mu \in \mathrm{Prob}(\Omega)$ minimizing the relaxed problem (3). The probability measure μ_N equidistributed on the set Γ_N approximates μ, hence we can expect the set Γ_N to also approximate $\mathrm{supp}(\mu)$. The quantization dimension $D_{\mathrm{quant}}(\mu)$ is difficult to estimate, but by Proposition 4.2 it admits the simpler upper bound $D_{\mathrm{box}}(\mathrm{supp}(\mu))$. We estimate the latter by applying the furthest point sampling algorithm to the finite metric space Γ_N, which defines an ordering on the elements of Γ_N as follows: let γ_1 be an arbitrary point of Γ_N and define by induction

$$\gamma_{i+1} := \arg \max_{\gamma \in \Gamma_N} d(\gamma, \{\gamma_1, \ldots, \gamma_i\}) \tag{28}$$

21

As in Definition 4.1, denote by $r_i = r_i(\Gamma_N)$ is the smallest $r \geq 0$ such that Γ_N can be covered by i balls of radius r. For $1 \ll i \ll N$, the ratio $\log(i)/\log(1/r_i(\Gamma_N))$ is expected to approximate $\log(i)/\log(1/r_i(\mathrm{supp}(\mu)))$ and thus the desired $D_{\mathrm{box}}(\mathrm{supp}\,\mu)$.

Lemma 5.3. *Let $\varepsilon_i := \max_{\gamma \in \Gamma} d(\gamma, \{\gamma_1, \ldots, \gamma_i\})$, where γ_i is defined as in* (28). *Then,*

$$\left(1 - \frac{\log(2)}{\log(1/\varepsilon_i)}\right) \frac{\log(i)}{\log(1/\varepsilon_i)} \leq \frac{\log(i)}{\log(1/r_i)} \leq \frac{\log(i)}{\log(1/\varepsilon_i)}$$

Proof. By construction, $r_i \leq \varepsilon_i$. Moreover, the balls centered at the points $\gamma_1, \ldots, \gamma_i$ and with radius $\varepsilon_i/2$ are disjoint, so that $r_i \geq \varepsilon_i/2$. $\qquad\square$

5.3 Test cases and numerical results

Our two testcases are constructed from two stationary solutions to Euler's equation in 2D. Let $s : \mathbb{R}_+ \to \mathbb{S}$ be a classical solution to Euler equation in Lagrangian coordinates (6), starting from the identity map. We solve the discretized version (9) of the minimization problem (2)-(3), with $s_* = s(0) = \mathrm{Id}$ and $s^* := s(t_{\max})$, where $t_{\max} > 0$. For small values of $t_{\max}$ the solution to this boundary problem is simply the original classical flow s, but for larger values a completely different generalized flow is obtained. In this case the geodesic s in the space of the measure preserving diffeomorphisms is no longer the unique shortest path between its boundary values s_* and s^*. The first classical behavior is guaranteed if the pressure hessian satisfies

$$\nabla^2 p \prec (\pi/t_{\max})^2 \, \mathrm{Id} \tag{29}$$

uniformly on $[0, t_{\max}] \times X$, see (7) and [Bre89]. In all the numerical experiments, the number of points is set to $N = 10\,000$ and the number of timesteps is $T = 2^4 + 1 = 17$.

5.3.1 Rotation of the disk

On the unit disk $D = \{(x_1, x_2) \in \mathbb{R}^2; x_1^2 + x_2^2 \leq 1\}$, the simplest stationary solution to Euler's equation (1) is given by a time-independent pressure field and speed:

$$p(x_1, x_2) = \frac{1}{2}(x_1^2 + x_2^2), \qquad\qquad v(x_1, x_2) = (-x_2, x_1).$$

The corresponding Lagrangian flow $s(t)$ is simply the rotation of angle t. The largest eigenvalue of $\nabla^2 p$ is 1 at every point in D. Hence by (29) the flow of rotations is the unique minimizer to both the variational formulation (2) and its relaxation (3) with boundary values $s_* = s(0) = \mathrm{Id}$ and $s^* = s(t_{\max})$, when $t_{\max} < \pi$. Uniqueness is lost at the critical time $t_{\max} = \pi$ which corresponds to a rotation of angle π, so that the final diffeomorphism becomes $s_* = s(\pi) = -\,\mathrm{Id}$. In this situation, the minimization problem (2) has two classical solutions, namely the clockwise and counterclockwise rotations. The relaxation (3) has uncountably many generalized solutions such as, by linearity, superpositions of these two rotations.

Another explicit example of generalized solution was discovered by Brenier [Bre89]: given a point $x \in D$ and a speed v, denote by $\omega_{x,v}$ the curve $\omega_{x,v}(t) = x\cos(t) + v\sin(t)$, $t \in [0, 1]$. Then, Brenier's solution is obtained as the pushforward by the map $(x, v) \mapsto \omega_{x,v} \in \Omega$ of the measure on $D \times \mathbb{R}^2$ defined by

$$\mu(dx, dv) = \frac{1}{\pi}\mathcal{H}^2(dx) \otimes \frac{1}{2\pi\sqrt{1 - |x|^2}} \, \mathcal{H}^1\big|_{\{|v| = \sqrt{1-|x|^2}\}}(dv),$$

where $\mathcal{H}^k$ denotes the k-dimensional Hausdorff measure. In particular, the quantization dimension of the solution is $3 = 2 + 1$. We refer to [BFS09] for more examples of optimal flows, and construct four dimensional one. Let μ_r be defined by combining (i) a classical rotation on the annulus $D \setminus D(r)$, with $D(r) = \{x \in \mathbb{R}^2; \ |x| \leq r\}$ and (ii) Brenier's solution rescaled by a factor r on the disc $D(r)$. Then μ_r is an optimal generalized flow of quantization dimension 3, whereas the averaged flow $\int_0^1 \mu_r dr$ is also optimal by linearity, and has quantization dimension 4.

Numerical results The numerical solutions computed by our algorithm for the critical time $t_{\max} = \pi$ are highly non-deterministic. To see this, we select a small neighborhood around several points in the unit disk D and look at the trajectories emanating from this small neighborhood. As shown in Figure 7, the trajectories emanating from each neighborhood at initial time tend to fill up the disk at intermediate times before gathering again on a small neighborhood at final time. In addition, each indivual trajectory looks like an ellipse, as in Brenier's explicit solution. Second, we estimate the box dimension of the support of the numerical solution (as explained in §5.2). The estimated dimension is slightly above 3.

5.3.2 Beltrami flow on the square

On the unit square $S = [-1/2, 1/2]^2$, we consider the Beltrami flow constructed from the time-independent pressure and speed:

$$p(x_1, x_2) = \frac{1}{2}(\sin(\pi x_1)^2 + \sin(\pi x_2)^2)$$
$$v(x_1, x_2) = (-\cos(\pi x_1)\sin(\pi x_2), \sin(\pi x_1)\cos(\pi x_2))$$

The maximum eigenvalue of the pressure Hessian $\nabla^2 p$ is π^2, and [Bre89] implies that the associated flow is minimizing between $s_* = s(0) = \mathrm{Id}$ and $s^* = s(t_{\max})$ for $t_{\max} \leq 1$. Because the square has much less symmetries than the disk, generalized solutions constructed from this flow are not as well understood as those occuring from rotations of the disk.

Numerical results Our numerical results suggest the following observations. First, as shown in Figure 9, the computed solutions with boundary values $s_* = \mathrm{Id}$ and $s^* = s(t_{\max})$ approximate the classical flow if $t_{\max} < 1$, and are non-deterministic generalized flows if $t_{\max} > 1$. This suggests the sharpness of the bound given by [Bre89]. Interestingly, even for $t_{\max} > 1$, the numerical solutions seem to remain deterministic in a neighborhood of the boundary of the cube. This can be seen more clearly in Figure 10, where the particles have been divided into clusters using the k-means algorithm (the clustering algorithm is explained in §5.2.2).

The pressure gradient is estimated as in §5.2.1 and is displayed in Figure 11. These pictures seem to indicate a loss of regularity of the pressure near the initial and final times. This corroborates the result of [AF07] according to which the pressure belongs to $L^2_{\mathrm{loc}}(]0, T[, \mathrm{BV}(X))$.

Figure 7 suggests that the even for $t_{\max} = 1.5$, the reconstructed solution for the Beltrami flow are more deterministic than the solution to the disk inversion. We estimate the box dimension of the support of the solution using the method explained in §5.2.2. The results are displayed in Figure 8. The estimated dimension is $D = 2$ for the deterministic solution ($t_{\max} = 0.9$) but it increases as the maximum time (and therefore the amount of non-determinism) increases. Finally, we note that the estimated dimensions for $t_{\max} \in \{1.1, 1.3, 1.5\}$ seem to be strictly between 2 and 3, suggesting a fractal structure for the support of the solution. This would need to be confirmed by a mathematical study.

Software. The software developed for generating the results presented in this article is publicly available at `https://github.com/mrgt/EulerSemidiscrete`

Acknowledgement The authors thank Y. Brenier for constructive discussions and introducing them to the topic of Euler equations of inviscid incompressible fluids.

(a) $(x,y) = (-0.7, 0)$ (b) $(x,y) = (-0.35, 0)$ (c) $(x,y) = (0, 0)$

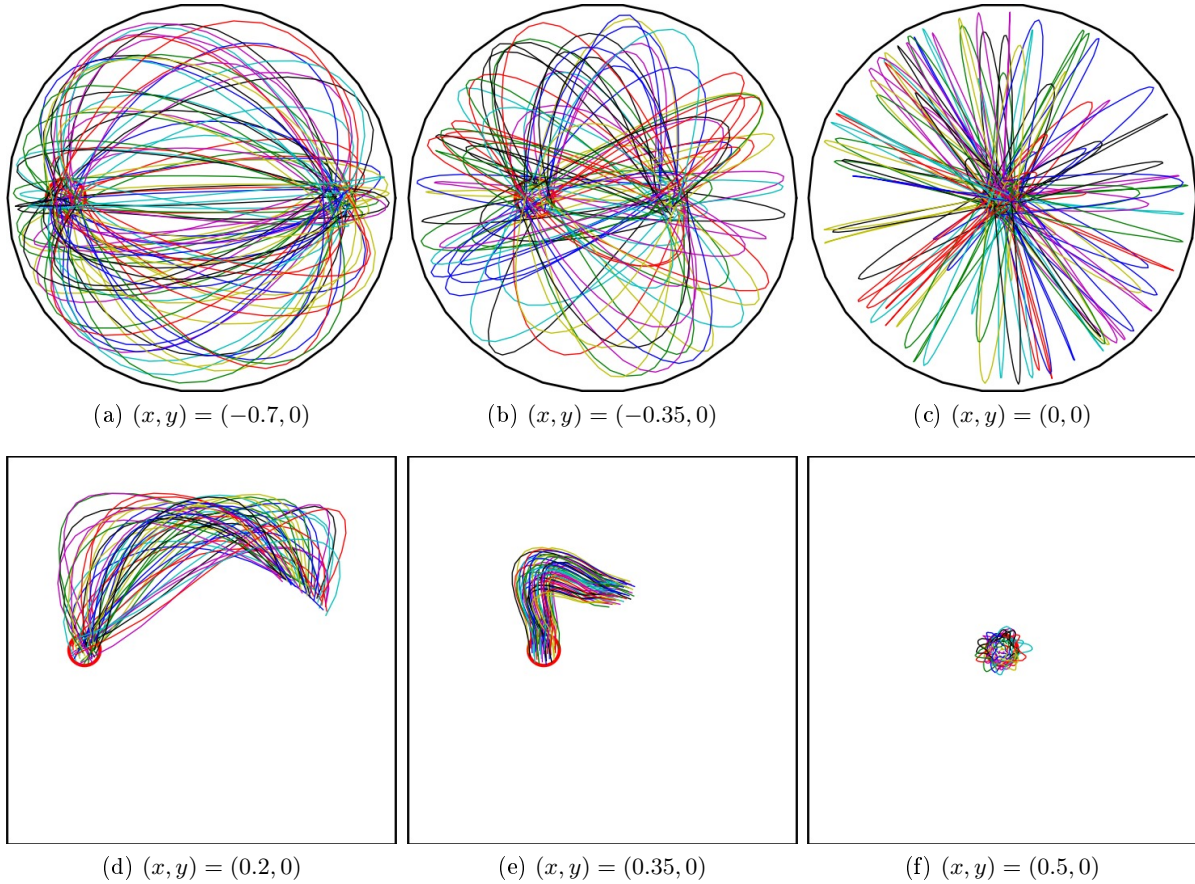(d) $(x,y) = (0.2, 0)$ (e) $(x,y) = (0.35, 0)$ (f) $(x,y) = (0.5, 0)$

Figure 7: We select particles whose initial position lie in a small disk, and display their trajectories according to the computed solution to (8). (Top) For the inversion of the unit disk (Bottom) For the Beltrami flow on the square, with $t_{\max} = 1.5$.

References

[AF07]   Luigi Ambrosio and Alessio Figalli. On the regularity of the pressure field of Brenier's weak solutions to incompressible Euler equations. *Calculus of Variations and Partial Differential Equations*, 2007.

[AHA98] F Aurenhammer, F Hoffmann, and B Aronov. Minkowski-Type Theorems and Least-Squares Clustering. *Algorithmica*, 1998.

[Arn66] Vladimir Arnold. Sur la géométrie différentielle des groupes de Lie de dimension infinie et ses applications à l'hydrodynamique des fluides parfaits. *Annales de l'institut Fourier*, 1966.
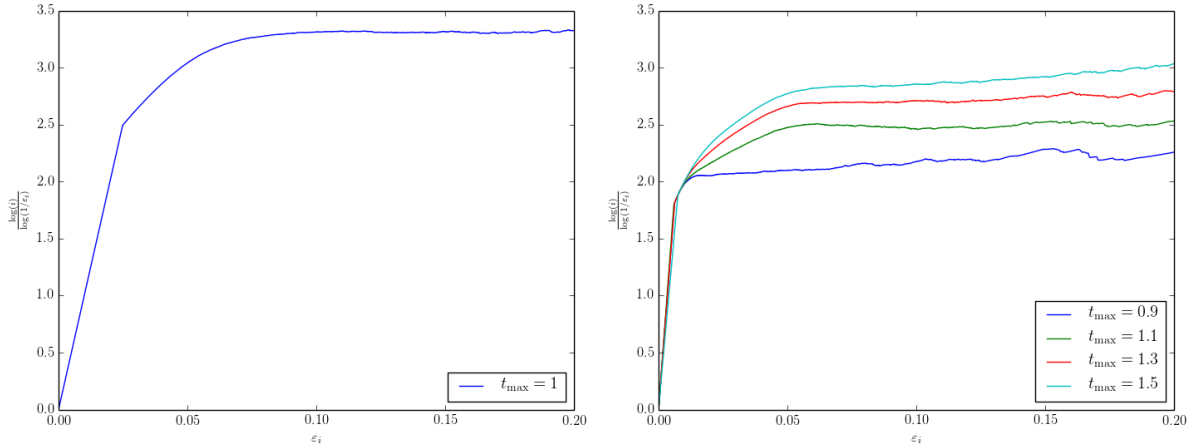
Figure 8: Estimation of the box counting dimension of the support of the computed solution, see §5.2.2. *(Left)* for the inversion of the unit disk *(Right)* Comparison between the estimated box counting dimensions of the solutions to the Beltrami flow on the square, depending on the maximum time.

[BBG02]   J D Benamou, Y Brenier, and K Guittet. The Monge-Kantorovitch mass transfer and its computational fluid mechanics formulation. *International Journal for Numerical Methods in Fluids*, 2002.

[BCC+15]   Jean-David Benamou, Guillaume Carlier, Marco Cuturi, Luca Nenna, and Gabriel Peyré. Iterative Bregman Projections for Regularized Transportation Problems. *SIAM Journal on Scientific Computing*, 37(2):A1111–A1138, January 2015.

[BCM14]   Jean-David Benamou, Francis Collino, and Jean-Marie Mirebeau. Monotone and Consistent discretization of the Monge-Ampere operator (Preprint). *arXiv.org*, 2014.

[BCMO14]   Jean-David Benamou, Guillaume Carlier, Q Merigot, and Edouard Oudet. Discretization of functionals involving the Monge-Ampère operator. *arXiv.org*, 2014.

[BFO14]   Jean-David Benamou, Brittany D Froese, and A M Oberman. Numerical solution of the Optimal Transportation problem using the Monge–Ampère equation. *Journal of Computational Physics*, 2014.

[BFS09]   Marc Bernot, Alessio Figalli, and Filippo Santambrogio. Generalized solutions for the Euler equations in one and two dimensions. *Journal de Mathématiques Pures et Appliquées*, 2009.

[BLNZ95]   Richard H Byrd, Peihuang Lu, Jorge Nocedal, and Ciyou Zhu. A limited memory algorithm for bound constrained optimization. *SIAM Journal on Scientific Computing*, 16(5):1190–1208, 1995.

[Bre89]   Yann Brenier. The least action principle and the related concept of generalized flows for incompressible perfect fluids. *Journal of the American Mathematical Society*, 1989.

[Bre91]   Yann Brenier. Polar factorization and monotone rearrangement of vector-valued functions. *Communications on Pure and Applied Mathematics*, 1991.
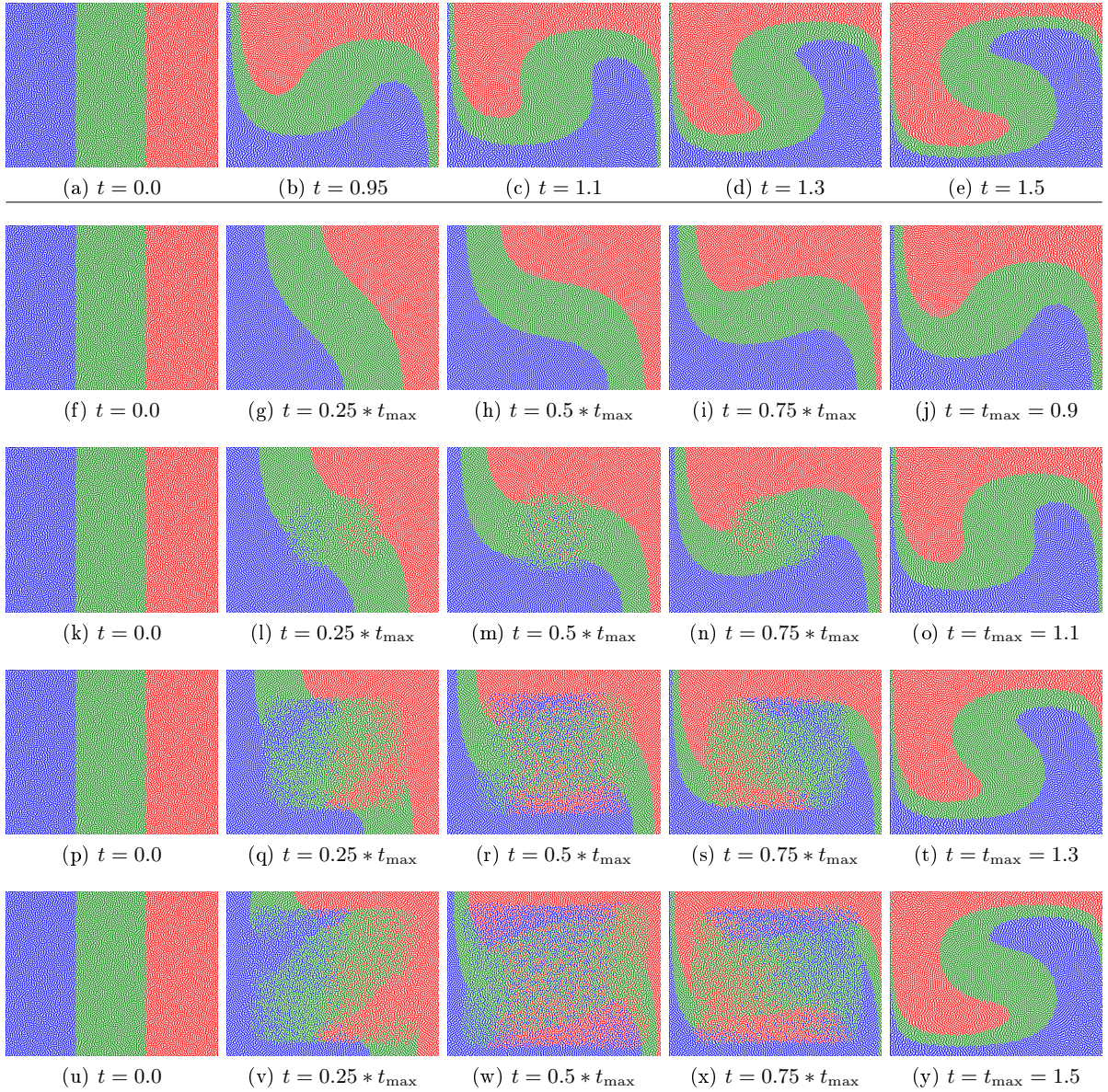
Figure 9: *(First row)* Beltrami flow in the unit square at various timesteps, a classical solution to Euler's equation. The color of the particles depend on their initial position. *(Second to fifth row)* Generalized fluid flows that are reconstructed by our algorithm, using boundary conditions displayed in the first and last column. When $t_{max} < 1$ we recover the classical flow, while for $t_{max} \geq 1$ the solution is not classical any more and includes some mixing.

[Bre93]   Y Brenier. The dual least action principle for an ideal, incompressible fluid . *Archive for rational mechanics and analysis*, 1993.

[Bre08]   Yann Brenier. Generalized solutions and hydrostatic approximation of the Euler equations. *Physica D. Nonlinear Phenomena*, 2008.

[Bre11]   Yann Brenier. A modified least action principle allowing mass concentrations for the early universe reconstruction problem. *Confluentes Mathematici*, 2011.
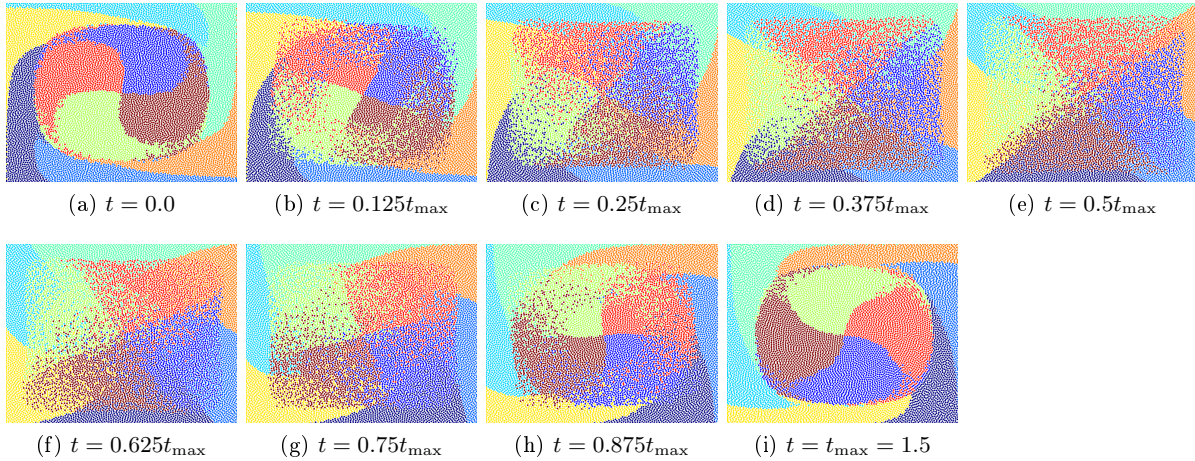
(a) $t = 0.0$ (b) $t = 0.125t_{\max}$ (c) $t = 0.25t_{\max}$ (d) $t = 0.375t_{\max}$ (e) $t = 0.5t_{\max}$

(f) $t = 0.625t_{\max}$ (g) $t = 0.75t_{\max}$ (h) $t = 0.875t_{\max}$ (i) $t = t_{\max} = 1.5$

Figure 10: Using the k-means cluster algorithm, we cluster the reconstructed trajectories for the Beltrami flow in the square with $t_{\max} = 1.5$ into 10 groups, whose particles are displayed with different collors. The resulting pictures suggest that close to the boundary of the square the movement of particle is clockwise and deterministic while in the interior the movement is highly non-deterministic and counter-clockwise.

[cga]   CGAL, Computational Geometry Algorithms Library. http://www.cgal.org.

[CL55]   Earl A Coddington and Norman Levinson. *Theory of ordinary differential equations*. Tata McGraw-Hill Education, 1955.

[CPR15]   Marco Cuturi, Gabriel Peyré, and Antoine Rolet. A Smoothed Dual Approach for Variational Wasserstein Problems. *arXiv.org*, March 2015.

[dGBOD12] Fernando de Goes, Katherine Breeden, Victor Ostromoukhov, and Mathieu Desbrun. Blue noise through optimal transport. *ACM Transactions on Graphics (TOG)*, 2012.

[Eul65]   Leonhard Euler. *Opera Omnia*. 1765.

[FD12]   Alessio Figalli and S Daneri. Variational models for the incompressible Euler equations. *HCDTE Lecture Notes, Part II*, 2012.

[GG92]   Allen Gersho and Robert M Gray. *Vector Quantization and Signal Compression*. Springer Science & Business Media, 1992.

[Lév14]   Bruno Lévy. A numerical algorithm for L_2 semi-discrete optimal transport in 3D. *arXiv.org*, 2014.

[Mer11]   Q Merigot. A Multiscale Approach to Optimal Transport. *Computer Graphics Forum*, 2011.

[OR15]   A M Oberman and Yuanlong Ruan. An efficient linear programming method for Optimal Transportation. *arXiv.org*, September 2015.

[PPO13]   Nicolas Papadakis, Gabriel Peyré, and Edouard Oudet. Optimal Transport with Proximal Splitting. *arXiv.org*, 2013.
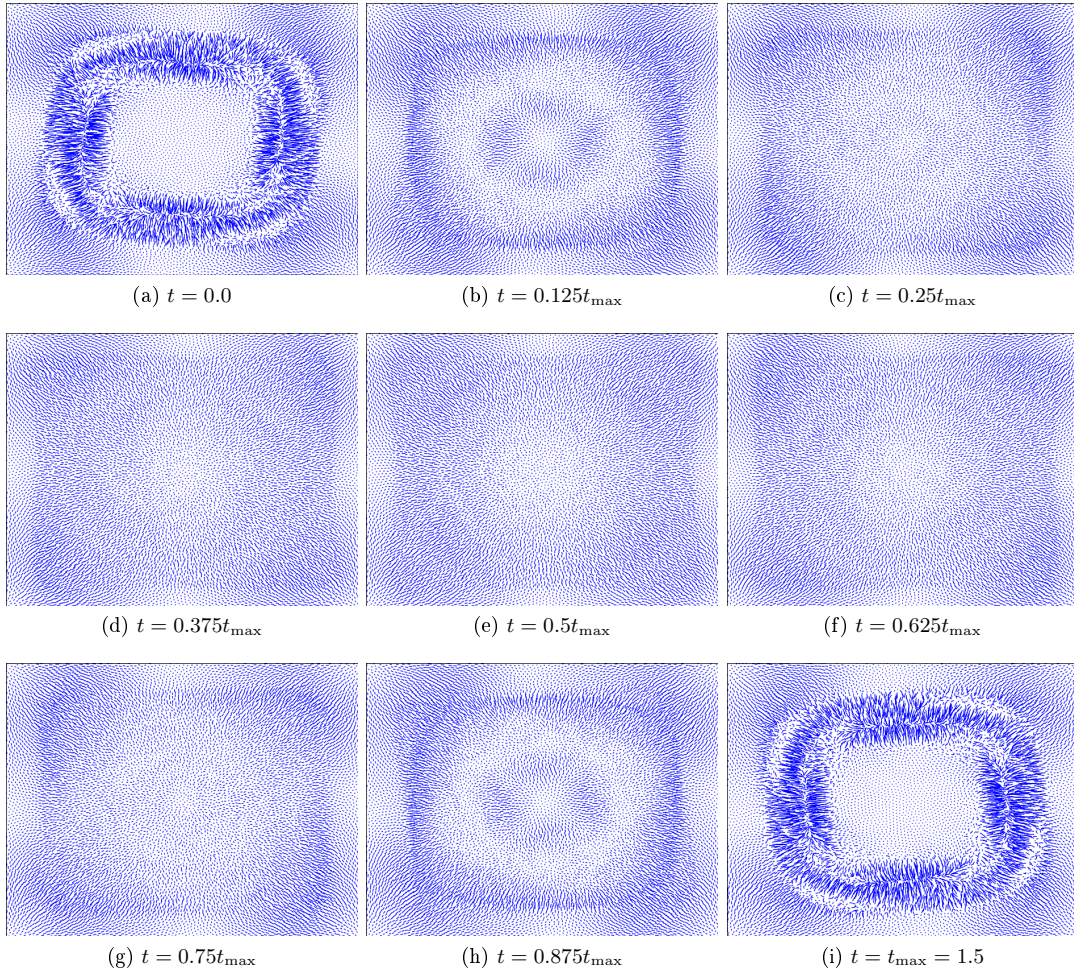
Figure 11: Estimated pressure gradient for the Beltrami flow on the square with $t_{\max} = 1.5$.

[Sch15]   Bernhard Schmitzer. A sparse algorithm for dense optimal transport. In Jean-François Aujol, Mila Nikolova, and Nicolas Papadakis, editors, *Scale Space and . . .*, pages 629–641. Springer International Publishing, 2015.

[Shn94]   A I Shnirelman. Generalized fluid flows, their approximation and applications. *Geometric and Functional Analysis*, 1994.

[Yvi13]   Mariette Yvinec. 2D triangulations. In *CGAL User and Reference Manual*. CGAL Editorial Board, 4.2 edition, 2013.